

Estimation of Population Size with Heterogeneous Catchability and Behavioural Dependence: Applications to Air and Water Borne Disease Surveillance

Kiranmoy Chatterjee* Prajamitra Bhuyan†

*Bidhannagar College Kolkata

†Department of Mathematics, Imperial College London, London

Abstract

Population size estimation based on the capture-recapture experiment is an interesting problem in various fields including epidemiology, criminology, demography, etc. In many real-life scenarios, there exists inherent heterogeneity among the individuals and dependency between capture and recapture attempts. A novel trivariate Bernoulli model is considered to incorporate these features, and the Bayesian estimation of the model parameters is suggested using data augmentation. Simulation results show robustness under model misspecification and the superiority of the performance of the proposed method over existing competitors. The method is applied to analyse real case studies on epidemiological surveillance. The results provide interesting insight on the heterogeneity and dependence involved in the capture-recapture mechanism. The methodology proposed can assist in effective decision-making and policy formulation.

Key words: COVID-19, Gibbs sampling, Hepatitis A, List dependence, Multiple systems estimation.

1 Introduction

The knowledge about the true prevalence of a disease in a specified period is an essential requirement for surveillance and effective policy formulation regarding the healthcare system of a state (Bird and King, 2018). In general, the available data source fails to cover all the relevant events and that leads to an undercount of the target population suffering from the disease. Therefore, disease ascertainment data are accumulated from multiple sources to increase the coverage and for the estimation of the disease prevalence (Papoz et al., 1996). This method is

known as multiple system estimation (MSE) which is equivalent to the capture-mark-recapture (CMR) method traditionally applied to estimate the size of wildlife populations (Hook and Regal, 1995; International Working Group for Disease Monitoring and Forecasting, 1995). The MSE is also popularly used for the estimation of demographic counts such as births and deaths (O'Hara et al., 2009), census undercoverage (Zaslavsky and Wolfgang, 1993), crime incidence (Cruyff et al., 2017), number of beneficiaries in a welfare economic study (Bird and King, 2018), etc. Lately, the MSE is also applied in clinical settings for screening and preventive studies (Bohning and Heijden, 2009).

The MSE involves the matching of the individuals enlisted from different sources and recording the various forms of overlaps among these lists. Traditionally two sources are considered, and it is a common practice to assume the independence between the lists for the estimation of population size which in many cases affected by correlation bias when the underlying assumption fails (ChandraSekar and Deming, 1949). In most cases, these sources of information are dependent because an individual's behaviour changes with the time of subsequent recapture attempts after the initial attempt. Another possible reason for dependence between lists is that capture probability may vary across individuals in each list (Chao et al., 2001). Therefore, more than two data sources are considered to capture more eligible events and to assess the underlying interdependence among the lists. In particular, three samples or lists are commonly considered in epidemiological surveillance (Gallay et al., 2000; Van Hest, 2007; Ruche et al., 2013). Note that the population of interest is assumed closed during the ascertainment of events from the three sources which generally occurs within a short period. The data obtained from three different sources are summarized in the form of an incomplete 2^3 contingency table. This data structure, presented in Table A.1 (See Appendix A), is typically known as the triple record system (TRS). Denote the capture status of an event in the first, second, and third lists by i , j , and k , respectively. The dummy variables i , j , and k take value 1 for capture and 0 otherwise. The total number of events with a particular capture status, say (i, j, k) , is denoted by x_{ijk} . For example, the count x_{101} associated with the cell $(1, 0, 1)$ represents the number of events that appear in the first and the third lists but absent in the second list. Similarly, x_{000} represents the number of events that are not captured by any of the three sources and remains unknown. Therefore, the problem of estimating the population size $N = \sum_{i,j,k} x_{ijk}$ is equivalent to that of the unknown cell count x_{000} . Interested readers are referred to Zaslavsky and Wolfgang (1993); Chatterjee and Bhuyan (2020b) for a detailed discussion on TRS and as-

sociated estimation methodology. In this article, we consider the problem of estimating disease prevalence motivated by TRS data available from the following case studies on epidemiological surveillance related to fatal illness due to air and water borne bacteria and viruses.

1.1 Legionnaires' Disease

Legionnaires' Disease (LD) is an unusual variant of pneumonia that occurs sporadically and in outbreaks caused by the bacterium Legionella which spreads through airborne water droplets (Den et al., 2002b; Lettinga et al., 2002). The motivation for considering surveillance on LD is two-fold in light of the current pandemic of COVID-19. Firstly, reports of co-infection with respiratory pathogens are increasing throughout the world (Lai et al., 2020). Also, it has been reported that 50% of COVID-19 patients who succumbed had secondary bacterial infections like LD (Zhou et al., 2020). Secondly, patients with COVID-19 should be screened for LD because the signs and symptoms of both infections are similar. The scientific community very recently found that COVID-19 infections can predispose patients to Legionella co-infections and consequently pose a serious threat to high-risk COVID-19 patients, which can lead to an increase in the severity of LD and mortality (Dey and Ashbolt, 2020).

The Netherlands is one of the worst affected countries by LD in the world. We consider a study on LD in the Netherland conducted during the period from 2000 to 2001 (Van Hest et al., 2008). The average national annual incidence rate of LD was 1.4 patients per 100 thousand inhabitants of the Netherlands in 1999. But experts suspect that the conventional LD notification system contains false-positive cases and often incomplete for true positive cases of LD (Van Hest et al., 2008). In this regard, efficient record-linkage and capture-recapture analysis for assessing the quality and completeness of infectious disease registers are warranted. In this study, information on LD affected patients is collected from Disease Notifications Register (DNR) from the Health Care Inspectorate, Laboratory results, and Hospital admissions. In the DNR, 373 LD patients are identified through record linkage. On the other hand, a total of 261 patients with a positive test for LD are recorded from the Laboratory survey. In total, 663 patients are enlisted in the hospital records with a relatively large number of 332 patients captured exclusively in this list. The overlap counts associated with these three lists are provided in the Appendix A (See Table A.2). The presence of dominant interaction between the DNR and the Laboratory register has been indicated in a

previous study (Van Hest et al., 2008). Moreover, various factors like geographical region, age, and laboratory diagnostics technique cause heterogeneity in capture probabilities of the individuals in each list (Nardone et al., 2003; Den et al., 2002a).

1.2 Hepatitis A Virus

Viral hepatitis is among the top ten leading causes of mortality worldwide and is the only communicable disease where mortality is increasing (Brown et al., 2017). The hepatitis A virus (HAV) spreads through person-to-person contact and contaminated food or water. In high-income countries, HAV infection usually occurs among drug addicts, men having sex with men, including patients with HIV and other sexually transmitted infections due to a low prevalence of anti-HAV antibodies (Cuthbert, 2001; Chen et al., 2019). In the scientific community opine that continuous HAV surveillance and evaluation of long-term vaccine effectiveness among HIV patients are warranted and HAV vaccination for all at childhood will provide more sustainable immunity in the general population. Therefore, it is important to know the actual population size infected with HAV for efficient vaccination policy and disease surveillance.

Approximately 1.4 million infections are reported worldwide each year, of which approximately half occur in Asian countries (Martin and Lemon, 2006). In particular, Taiwan has a history of a high prevalence of HAV infection because of indigenous townships with inadequate water, sanitation, and hygiene infrastructure in the last decade of the twentieth century (Chen et al., 2019). We consider a study on HAV outbreak in northern Taiwan from April to July 1995 near a technical college (Chao et al., 1997). There are three registered sources of information on the HAV infected college students available: (i) P-list consists of 135 records based on a serum test taken by the Institute of Preventive Medicine, Department of Health of Taiwan, (ii) Q-list includes 122 cases reported by doctors in local hospitals and this 10 list was provided by the National Quarantine Service and (iii) E-list comprise of 126 cases based on questionnaires conducted by epidemiologists. Tsay and Chao (2001) reported the existence of heterogeneity in capture probabilities in all three sources, and low overlap has been observed among the lists. The summarized data are provided in the Appendix A (See Table A.2).

1.3 The Challenges in Analysing TRS Data

As mentioned before, the assumption of list independence is often violated in practice mainly due to two reasons: (i) list dependence caused by behavioral response variation, i.e. the inclusion status of an individual in one list has a direct causal effect on his/her inclusion status in other lists; (ii) the propensity to be captured in a list is heterogeneous over individuals (Chao et al., 2001). Even there is no behavioral response variation, the ascertainment of the sources may become dependent if the capture probabilities of the individuals are heterogeneous. In both the case studies discussed in Subsections 1.1-1.2, the TRS datasets are potentially affected by the list dependence because of these aforementioned causes. The dependencies arising from these two different mechanisms are usually confounded and cannot be easily disentangled in real applications (Chao, 2001). In the literature of multiple systems estimation, various models which account for the list dependence have been proposed to estimate N . In this context, Fienberg (1972b) proposed log-linear models and discussed associated estimation methodology. An overview of log-linear models and their applications for population size estimation is provided by Cormack (1989). However, it is important to note that the parameters that are associated with the log-linear models are not well interpretable for practitioners (Coumans et al., 2017). In the context of ecological surveillance, model M_{tb} is frequently used to account for the time and behavioural response variation (Otis et al., 1978). This model has several practical limitations (Chatterjee and Bhuyan, 2020a). See Appendix B.2 for more details. As mentioned before, list dependence may exist due to heterogeneity among the individuals in the absence of behavioral response variation. In such cases, the quasi-symmetric or partial quasi-symmetric Rasch models are widely used to estimate the population size (Rasch, 1961). The most general scenario of the capture-recapture experiment encompasses all the three sources of variation - time/list variation, individual heterogeneity, and behavioral response variation in the capture probabilities of the individuals in the population of interest. In this context, modeling of the TRS data is a challenging task (Chao et al., 2001), and such a complex scenario may often arise in various fields of applications including epidemiology (Tsay and Chao, 2001; Van Hest et al., 2008). Chao and Tsay (1998) proposed a non-parametric estimate of N based on the sample coverage approach. However, the performance of this method is not satisfactory and it may provide infeasible estimates. See Appendix B.4 and Section 4 for details.

In this article, we propose a novel modeling approach based on the trivariate Bernoulli

model that incorporates both the behavioral dependencies between the lists and the individual heterogeneity along with the list variation. The model parameters are easily interpretable and provide interesting insights into the capture-recapture mechanism. We develop a Bayesian estimation methodology for the estimation of N and associated model parameters. In particular, we demonstrate how Gibbs sampling facilitates Bayesian analyses of capture-recapture experiments in the most general scenario. As a result, formulations that were previously avoided because of analytical intractability and computational time can now be easily considered for practical applications. The description of the proposed model and its special cases are provided in Section 2. In Section 3, estimation methodologies for the population size N and associated model parameters are discussed. Next, the performance of the proposed method is compared with the existing competitors through an extensive simulation in Section 4. Sensitivity analyses concerning prior choices and model misspecifications are also discussed in the same section. Analyses of real datasets on LD and HAV are presented in Section 5. We summarise the key findings and conclude with some discussion on future research in Section 6.

2 Modeling Individual Heterogeneity and List Dependence

In this section, we first discuss the Trivariate Bernoulli model (TBM) proposed by [Chatterjee and Bhuyan \(2020a\)](#) for modeling capture–recapture data under TRS. The TBM is used to incorporate the inherent list dependence, and its parameters possess physical interpretation. We extend this model in a more general setup to account for the ‘individual heterogeneity’ in addition to the list dependence.

In TRS, some individuals behave independently over the three different capture attempts and behavioural dependence exists for the rest of the population. To model the association among the three lists L_1 , L_2 and L_3 , we first consider that α_1 , α_2 , and α_3 proportion of individuals possess pairwise dependence between lists $(L_1 \text{ and } L_2)$, $(L_2 \text{ and } L_3)$ and $(L_1 \text{ and } L_3)$. Further, we consider the second-order dependency among the three lists L_1 , L_2 and L_3 for α_4 proportion of individuals. Therefore, the remaining $(1 - \alpha_0)$ proportion of individuals, where $\alpha_0 = \sum_{l=1}^4 \alpha_s$, behave independently over the three lists. Now we define a triplet $(X_{1h}^*, X_{2h}^*, X_{3h}^*)$ which represents the latent capture statuses of the h th individual in the first,

second and third attempts respectively, for $h = 1, 2, \dots, N$. The latent capture status X_{lh}^* takes value 1 or 0, denoting the presence or absence of the h th individual in the l th list, for $l = 1, 2, 3$. Under this setup, $X_{2h}^* = X_{1h}^*$ and $X_{3h}^* = X_{2h}^*$ for α_l and α_2 proportion of individuals, respectively. Similarly, $X_{3h}^* = X_{1h}^*$ for α_3 proportion of individuals, and $X_{3h}^* = X_{2h}^* = X_{1h}^*$ for α_4 proportion of individuals. Now, denote $Z_h^{(1)}$, $Z_h^{(2)}$, and $Z_h^{(3)}$ as the the inclusion statuses of the h th individual in L_1 , L_2 , and L_3 respectively, for $h = 1, 2, \dots, N$. Therefore, we can formally write the model to account the interdependencies among the three lists as:

$$(Z_h^{(1)}, Z_h^{(2)}, Z_h^{(3)}) = \begin{cases} (X_{1h}^*, X_{2h}^*, X_{3h}^*) & \text{with prob. } 1 - \alpha_0, \\ (X_{1h}^*, X_{1h}^*, X_{3h}^*) & \text{with prob. } \alpha_1, \\ (X_{1h}^*, X_{2h}^*, X_{2h}^*) & \text{with prob. } \alpha_2, \\ (X_{1h}^*, X_{2h}^*, X_{1h}^*) & \text{with prob. } \alpha_3, \\ (X_{1h}^*, X_{1h}^*, X_{1h}^*) & \text{with prob. } \alpha_4, \end{cases} \quad (1)$$

where X_{1h}^* 's, X_{2h}^* 's and X_{3h}^* 's are independently distributed Bernoulli random variables with parameters \mathcal{P}_1 , \mathcal{P}_2 and \mathcal{P}_3 , respectively, for all $h = 1, \dots, N$. Note that \mathcal{P}_l refers to the capture probability of a causally independent individual in the l th list. To incorporate heterogeneity in capture probabilities, we now consider X_{1h}^* 's to follow independent Bernoulli distributions with parameter \mathcal{P}_{lh} and model it as:

$$\text{logit}(\mathcal{P}_{lh}) = \log \left(\frac{\mathcal{P}_{lh}}{1 - \mathcal{P}_{lh}} \right) = b_{lh}, \quad h = 1, \dots, N, \quad (2)$$

where b_{lh} 's are independent and identically distributed realizations of random effect b_l , for each $l = 1, 2, 3$. We also assumes b_l 's are independently distributed. We refer this generic model, given in (1) and (2), as Trivariate Heterogeneous Bernoulli model (THBM).

2.1 Special Cases

The generic form of the proposed THBM incorporates the list variation, individual heterogeneity, and behavioral dependence arising from different sources. However, in some cases, the effect of the behavioral response variation is confounded due to heterogeneous catchability and may not provide additional information for the estimation of N . In such cases, it is prudent to consider a parsimonious model with some restrictions on the THBM. In particular, one

can consider $\alpha_s = 0$, for $s = 1, \dots, 4$, and this reduced model is applicable for the scenarios where the generalized Rasch model is useful (Darroch et al., 1993; Chao and Tsay, 1998) (See Appendix B.3). One can further assume b_l 's are identically distributed where the catchability of the individuals are the same irrespective of the lists. The THBM model reduces to TBM when b_l 's are degenerate random variables. This model is useful for TRS when the individuals are equally catchable in each list. As discussed in Chatterjee and Bhuyan (2020a), the TBM can be further reduced to submodels TBM-1 and TBM-2 if we consider $\alpha_3 = 0$ and $\alpha_4 = 0$, respectively. In the absence of list dependence (i.e. $\alpha_s = 0$, for $s = 1, \dots, 4$) the TBM and the M_t model are equivalent (Otis et al., 1978).

3 Estimation Methodology

A classical approach for estimating N in the context of CMR is based on the likelihood theory, where the vector of observed cell counts $\mathbf{x} = \{x_{ijk} : i, j, k = 0, 1; i = j = k \neq 0\}$ (as presented in Table A.1) follow a multinomial distribution with index parameter N and the associated cell probabilities $\mathbf{p} = \{p_{ijk} : i, j, k = 0, 1; i = j = k \neq 0\}$ (Sanathanan, 1972). Therefore, the likelihood function is given by

$$L(N, \mathbf{p} | \mathbf{x}) = \frac{N!}{\prod_{i,j,k=0,1; i=j=k \neq 0} x_{ijk}!(N - x_0)!} \prod_{i,j,k=0,1} p_{ijk}^{x_{ijk}},$$

where $x_{000} = N - x_0$. The TBM is characterized by the parameters $N, \alpha_1, \alpha_2, \alpha_3, \alpha_4, \mathcal{P}_1, \mathcal{P}_2, \mathcal{P}_3$, and using its relationships with the cell probabilities p_{ijk} , the likelihood function is given

by

$$\begin{aligned}
L(N, \boldsymbol{\alpha}, \boldsymbol{\mathcal{P}} | \mathbf{x}) \propto & \frac{N!}{(N - x_0)!} [(1 - \alpha_0)\mathcal{P}_1\mathcal{P}_2\mathcal{P}_3 + \alpha_1\mathcal{P}_1\mathcal{P}_3 + \alpha_2\mathcal{P}_1\mathcal{P}_2 + \alpha_3\mathcal{P}_1\mathcal{P}_2 + \alpha_4\mathcal{P}_1]^{x_{111}} \\
& \times [(1 - \alpha_0)\mathcal{P}_1\mathcal{P}_2(1 - \mathcal{P}_3) + \alpha_1\mathcal{P}_1(1 - \mathcal{P}_3)]^{x_{110}} \\
& \times [(1 - \alpha_0)(1 - \mathcal{P}_1)\mathcal{P}_2\mathcal{P}_3 + \alpha_2(1 - \mathcal{P}_1)\mathcal{P}_2]^{x_{011}} \\
& \times [(1 - \alpha_0)\mathcal{P}_1(1 - \mathcal{P}_2)(1 - \mathcal{P}_3) + \alpha_2\mathcal{P}_1(1 - \mathcal{P}_2)]^{x_{100}} \\
& \times [(1 - \alpha_0)\mathcal{P}_1(1 - \mathcal{P}_2)\mathcal{P}_3 + \alpha_3\mathcal{P}_1(1 - \mathcal{P}_2)]^{x_{101}} \\
& \times [(1 - \alpha_0)(1 - \mathcal{P}_1)\mathcal{P}_2(1 - \mathcal{P}_3) + \alpha_3(1 - \mathcal{P}_1)\mathcal{P}_2]^{x_{010}} \\
& \times [(1 - \alpha_0)(1 - \mathcal{P}_1)(1 - \mathcal{P}_2)\mathcal{P}_3 + \alpha_1(1 - \mathcal{P}_1)\mathcal{P}_3]^{x_{001}} \\
& \times [(1 - \alpha_0)(1 - \mathcal{P}_1)(1 - \mathcal{P}_2)(1 - \mathcal{P}_3) + \alpha_1(1 - \mathcal{P}_1)(1 - \mathcal{P}_3) \\
& \quad + \alpha_2(1 - \mathcal{P}_1)(1 - \mathcal{P}_2) + \alpha_3(1 - \mathcal{P}_1)(1 - \mathcal{P}_2) + \alpha_4(1 - \mathcal{P}_1)]^{N - x_0}, \tag{3}
\end{aligned}$$

where $x_{000} = N - x_0$, $p_{000} = 1 - \sum_{i,j,k=0,1; i=j=k \neq 0} p_{ijk}$, $\boldsymbol{\alpha} = (\alpha_1, \alpha_2, \alpha_3, \alpha_4)$, and $\boldsymbol{\mathcal{P}} = (\mathcal{P}_1, \mathcal{P}_2, \mathcal{P}_3)$. In contrast to TBM, the proposed THBM accounts for the ‘individual heterogeneity’ in terms of the variations in capture probabilities considering $\mathcal{P}_l = \frac{\exp(b_l)}{1 + \exp(b_l)}$ as a function of random effects b_l for $l = 1, 2, 3$. Now, integrating the likelihood function, given in (3), with respect to the distribution of random effects b_l , we obtain the marginal likelihood function of $\boldsymbol{\theta}$ as

$$L(\boldsymbol{\theta} | \mathbf{x}) = \int_{\mathbb{R}^3} L(N, \boldsymbol{\alpha}, \boldsymbol{\mathcal{P}} | \mathbf{x}) \times \left\{ \prod_{l=1}^3 g_{b_l}(b_l | \delta_l) \right\} db_1 db_2 db_3, \tag{4}$$

where $g_{b_l}(\cdot | \delta_l)$ is the density of b_l ’s with parameter δ_l for $l = 1, 2, 3$, and $\boldsymbol{\theta} = (N, \boldsymbol{\alpha}, \boldsymbol{\delta})$. In the conventional frequentist approach, computational challenges arise in the model fitting due to intractable numerical integration involved in the aforementioned log-likelihood function (Coul and Agresti, 1999). One can consider quasi-likelihood approaches or approximation methods for numerical integration using Gaussian quadrature or Laplace’s method. Alternatively, a Bayesian estimate of the parameters of interest can be obtained using the Metropolis-Hastings algorithm.

3.1 Identifiability Issues

The model parameters associated with THBM are not identifiable with respect to a TRS data. In a frequentist setup, the performance of point estimation in the absence of identifiability may

yield unsatisfactory results such as non-uniqueness of maximum likelihood estimates (White, 1982; Aldrich, 2002). To avoid the issues related to identifiability, Chatterjee and Bhuyan (2020a) considered two submodels TBM-1 and TBM-2 of TBM keeping α_3 and α_4 fixed as 0, respectively. Similar restrictions on parameters are also considered in the model M_{tb} and log-linear models as well as in the sample coverage approach proposed by Chao and Tsay (1998). However, this process of model contraction may lead to a model that involves dubious assumptions or a model that is less realistic in some other way (Gustafson, 2005). For example, available sources in epidemiological surveillance are not time ordered (Chao et al., 2001), and the capture attempts are supposed to be interdependent between themselves (Tsay and Chao, 2001; Ruche et al., 2013). Hence, the dependence between the first and third lists may be present, unlike the situation that is modelled by TBM-1. Similarly, TBM-2 is not suitable for the scenarios when the second-order interaction among the lists is present. On the other hand, non-identifiability is not seen as a big obstacle to perform inferential procedures in the Bayesian paradigm (Wechsler et al., 2013). The infusion of crude prior information into a non-identifiable model is considered as an alternative to achieve identifiability through model contraction. It is important to note that a non-identifiable model may bring information about the parameters of interest, and identifiable models do not necessarily lead to better decision making than non-identifiable ones (Gustafson, 2005; Wechsler et al., 2013). In the following subsection, we propose a Bayesian estimation methodology of the parameter of interest N and associated parameters of the THBM under different choices of prior specification on the nuisance parameters. Later, we also demonstrate that the proposed estimate of N is not sensitive to those prior specifications and outperforms existing competitors through an extensive simulation study (See Section 4).

3.2 Bayesian Approach

We propose a Bayesian estimation of the model parameters involved in the THBM given by (1) and (2), using the MCMC algorithm based on data augmentation. Unlike the usual frequentist set-up, the proposed Bayesian approach provides a natural framework for prediction over unobserved data. Thus, by generating posterior predictive densities, rather than point estimates, we can make probability statements giving greater flexibility in presenting results. For instance, we can discuss findings concerning specific hypotheses or in terms of credible

intervals which can offer a more intuitive understanding for the practitioners.

As mentioned before, the likelihood function $L(\boldsymbol{\theta}|\mathbf{x})$, given by (4), is not mathematically tractable due to involvement of an integral and the additive structure of the cell probabilities p_{ijk} impose further challenges. One can apply the Metropolis-Hastings algorithm to generate samples from the posterior distribution of the model parameters $\boldsymbol{\theta}$, however such computationally intensive methods are time inefficient and not appealing for the practitioners. To avoid such difficulty, we first attempt to simplify the likelihood function taking cue from the data augmentation strategy as suggested by [Tanner and Wong \(1987\)](#). For this purpose, we partition the observed cell counts x_{ijk} depending on the various types of list dependence as described in (1), and define a vector of latent cell counts as:

$$\mathbf{y} = \left\{ y_{ijk,u} : \sum_{l=1}^{\nu} y_{ijk,u} = x_{ijk}; i, j, k = 0, 1; \nu = 5^{\omega} 3^{1-\omega}; \omega = \mathbb{I}[i = j = k] \right\}.$$

where $\mathbb{I}[\cdot]$ is an indicator function. We also treat the random effects $\mathbf{b} = (b_1, b_2, b_3)$ as unobserved data. Therefore, the likelihood function of $\boldsymbol{\theta}$, based on the complete data $(\mathbf{x}, \mathbf{y}, \mathbf{b})$, is given by

$$\mathcal{L}_c(\boldsymbol{\theta}|\mathbf{x}, \mathbf{y}, \mathbf{b}) = \mathcal{L}_c(N, \boldsymbol{\alpha}, \mathbf{b}|\mathbf{x}, \mathbf{y}) \times \left\{ \prod_{l=1}^3 g_{b_l}(b_l|\delta_l) \right\}, \quad (5)$$

where

$$\begin{aligned} \mathcal{L}_c(N, \boldsymbol{\alpha}, \mathbf{b}|\mathbf{x}, \mathbf{y}) \propto & \frac{N!}{(N-x_0)!} [(1-\alpha_0)\mathcal{P}_1\mathcal{P}_2\mathcal{P}_3]^{y_{111,1}} \times [\alpha_1\mathcal{P}_1\mathcal{P}_3]^{y_{111,2}} \times [\alpha_2\mathcal{P}_1\mathcal{P}_2]^{y_{111,3}} \times [\alpha_3\mathcal{P}_1\mathcal{P}_2]^{y_{111,4}} \\ & \times [\alpha_4\mathcal{P}_1]^{x_{111}-\sum_{i=1}^4 y_{111,i}} \times [(1-\alpha_0)\mathcal{P}_1\mathcal{P}_2(1-\mathcal{P}_3)]^{y_{110,1}} \times [\alpha_1\mathcal{P}_1(1-\mathcal{P}_3)]^{x_{110}-y_{110,1}} \\ & \times [(1-\alpha_0)(1-\mathcal{P}_1)\mathcal{P}_2\mathcal{P}_3]^{y_{011,1}} \times [\alpha_2(1-\mathcal{P}_1)\mathcal{P}_2]^{x_{011}-y_{011,1}} \\ & \times [(1-\alpha_0)\mathcal{P}_1(1-\mathcal{P}_2)(1-\mathcal{P}_3)]^{y_{100,1}} \times [\alpha_2\mathcal{P}_1(1-\mathcal{P}_2)]^{x_{100}-y_{100,1}} \\ & \times [(1-\alpha_0)\mathcal{P}_1(1-\mathcal{P}_2)\mathcal{P}_3]^{y_{101,1}} \times [\alpha_3\mathcal{P}_1(1-\mathcal{P}_2)]^{x_{101}-y_{101,1}} \\ & \times [(1-\alpha_0)(1-\mathcal{P}_1)\mathcal{P}_2(1-\mathcal{P}_3)]^{y_{010,1}} \times [\alpha_3(1-\mathcal{P}_1)\mathcal{P}_2]^{x_{010}-y_{010,1}} \\ & \times [(1-\alpha_0)(1-\mathcal{P}_1)(1-\mathcal{P}_2)\mathcal{P}_3]^{y_{001,1}} \times [\alpha_1(1-\mathcal{P}_1)\mathcal{P}_3]^{x_{001}-y_{001,1}} \\ & \times [(1-\alpha_0)(1-\mathcal{P}_1)(1-\mathcal{P}_2)(1-\mathcal{P}_3)]^{y_{000,1}} \times [\alpha_1(1-\mathcal{P}_1)(1-\mathcal{P}_3)]^{y_{000,2}} \\ & \times [\alpha_2(1-\mathcal{P}_1)(1-\mathcal{P}_2)]^{y_{000,3}} \times [\alpha_3(1-\mathcal{P}_1)(1-\mathcal{P}_2)]^{y_{000,4}} \times [\alpha_4(1-\mathcal{P}_1)]^{N-x_0-\sum_{i=1}^4 y_{000,i}}. \end{aligned}$$

Interestingly, the complete data likelihood, given by (5), possesses a simple form as a product of the power functions of the parameters associated with the THBM. Hence, the joint posterior density of all the unobserved quantity in the model $\boldsymbol{\theta}$, \mathbf{y} , and \mathbf{b} given the observed data \mathbf{x} is provided by

$$\pi(\boldsymbol{\theta}, \mathbf{b}, \mathbf{y} | \mathbf{x}) \propto \mathcal{L}_c(\boldsymbol{\theta} | \mathbf{x}, \mathbf{y}, \mathbf{b}) \times \pi(\boldsymbol{\theta}), \quad (6)$$

where $\pi(\boldsymbol{\theta})$ denotes the prior for $\boldsymbol{\theta}$. Following [Tanner and Wong \(1987\)](#), we employ a simple iterative algorithm to generate samples from the posterior density of $\boldsymbol{\theta}$. To implement the following steps, one must be able to sample from the conditional posterior distributions of $\boldsymbol{\theta}$ given $(\mathbf{x}, \mathbf{y}, \mathbf{b})$, \mathbf{y} given $(\boldsymbol{\theta}, \mathbf{x}, \mathbf{b})$, and \mathbf{b} given $(\boldsymbol{\theta}, \mathbf{x}, \mathbf{y})$, denoted by $\pi(\boldsymbol{\theta} | \mathbf{x}, \mathbf{y}, \mathbf{b})$, $\pi(\mathbf{y} | \boldsymbol{\theta}, \mathbf{x}, \mathbf{b})$, and $\pi(\mathbf{b} | \boldsymbol{\theta}, \mathbf{x}, \mathbf{y})$, respectively.

Step 1. Set $t = 0$ and initialize $(\mathbf{y}^{(t)}, \mathbf{b}^{(t)})$.

Step 2. Generate $\boldsymbol{\theta}^{(t+1)}$ from $\pi(\boldsymbol{\theta} | \mathbf{x}, \mathbf{y}^{(t)}, \mathbf{b}^{(t)})$.

Step 3. Generate $\mathbf{y}^{(t+1)}$ from $\pi(\mathbf{y} | \boldsymbol{\theta}^{(t+1)}, \mathbf{x}, \mathbf{b}^{(t)})$, and then $\mathbf{b}^{(t+1)}$ from $\pi(\mathbf{b} | \boldsymbol{\theta}^{(t+1)}, \mathbf{x}, \mathbf{y}^{(t+1)})$.

Step 4. Update $(\mathbf{y}^{(t)}, \mathbf{b}^{(t)})$ with $(\mathbf{y}^{(t+1)}, \mathbf{b}^{(t+1)})$.

Step 5. Repeat Step 2-4 until convergence of $\left\{ \boldsymbol{\theta}^{(t)} \right\}_{t \geq 0}$.

Note that the conditional distribution $\pi(\mathbf{y} | \boldsymbol{\theta}, \mathbf{x}, \mathbf{b})$ of the unobserved data \mathbf{y} , is expressed as a product of Multinomial and Binomial distributions. See [Appendix C.1](#) for details. Now, one can easily execute the above steps using Gibbs sampling if the full conditional distributions of \mathbf{b} and $\boldsymbol{\theta}$ can be obtained in closed forms. In the next subsection, we propose appropriate priors for $\boldsymbol{\theta}$ and suitable distribution of the random effects \mathbf{b} , so that the conditional posteriors $\pi(\boldsymbol{\theta} | \mathbf{b}, \mathbf{y}, \mathbf{x})$ and $\pi(\mathbf{b} | \boldsymbol{\theta}, \mathbf{y}, \mathbf{x})$ result in standard distributions.

3.2.1 Prior Specifications

We first assume the random effect b_l follows generalized logistic type-I distribution ([Fischer, 2000](#)) with shape parameter δ_l for $l = 1, 2, 3$. This is among the few distributions which can

model both positively and negatively skewed data on the whole real line. With this specific choice of distribution, the conditional posterior distribution of \mathbf{b} given $(\boldsymbol{\theta}, \mathbf{x}, \mathbf{y})$ is obtained as

$$\pi(b_l | \boldsymbol{\theta}, \mathbf{x}, \mathbf{y}) \propto EGB2(n_l + 1, m_l + \delta_l), \quad l = 1, 2, 3,$$

where $EGB2$ denotes for exponential generalized beta distribution of second kind (Fischer, 2000) with parameters involving $m_1 = x_{1..}$, $m_2 = y_{111,1} + y_{111,3} + y_{111,4} + y_{110,1} + x_{011} + x_{010}$, $m_3 = y_{111,1} + y_{111,2} + y_{011,1} + y_{101,1} + x_{001}$, $n_1 = N - x_{1..}$, $n_2 = x_{100} + x_{101} + y_{001,1} + y_{000,1} + y_{000,3} + y_{000,4}$, and $n_3 = x_{110} + y_{100,1} + y_{010,1} + y_{000,1} + y_{000,2}$. See Appendix C.2 for detailed derivation. Now, one can easily sample from $\pi(b_l | \boldsymbol{\theta}, \mathbf{x}, \mathbf{y})$ and compute $\mathcal{P}_l = [1 + \exp(-b_l)]^{-1}$ for $l = 1, 2, 3$.

For our analysis, the prior on N , $\boldsymbol{\alpha}$, and $\boldsymbol{\delta}$ are assigned independently, i.e. $\pi(\boldsymbol{\theta}) = \pi(N)\pi(\boldsymbol{\alpha})\pi(\boldsymbol{\delta})$. We propose both informative and noninformative priors for the nuisance parameters $\boldsymbol{\alpha}$ and $\boldsymbol{\delta}$ with noninformative prior on the parameters of interest N . These different prior choices enable us to study the robustness of the proposed inferential methodology and provide flexibility to the users. The two different choices of the priors and associated conditional posterior distribution of $\boldsymbol{\theta}$ are provided below.

Prior Choice I

As discussed before, we first consider non-informative priors for the purpose of Bayesian estimation. The Jeffrey's prior for all the parameters involved in THBM are given by $\pi(N) \propto N^{-1}$, $\pi(\boldsymbol{\alpha}) \propto Dirichlet(0.5, 0.5, 0.5, 0.5, 0.5)$, and $\pi(\delta_l) \propto \delta_l^{-1}$ for $l = 1, 2, 3$. Under these choices, the full conditional densities of $\boldsymbol{\alpha}$ and δ_l 's are obtained as

$$\begin{aligned} \pi(\boldsymbol{\alpha} | \boldsymbol{\theta}_{-\boldsymbol{\alpha}}, \mathbf{x}, \mathbf{y}, \mathbf{b}) &\propto Dirichlet(\mathbf{d}), \\ \pi(\delta_l | \boldsymbol{\theta}_{-\delta_l}, \mathbf{x}, \mathbf{y}, \mathbf{b}) &\propto Exponential(w_l), \quad l = 1, 2, 3, \end{aligned}$$

where $\mathbf{d} = (d_1, d_2, d_3, d_4, d_5)$ with $d_1 = y_{111,2} + x_{110} - y_{110,1} + x_{001} - y_{001,1} + y_{000,2} + 0.5$, $d_2 = y_{111,3} + x_{011} - y_{011,1} + x_{100} - y_{100,1} + y_{000,3} + 0.5$, $d_3 = y_{111,4} + x_{101} - y_{101,1} + x_{010} - y_{010,1} + y_{000,4} + 0.5$, $d_4 = x_{111} - \sum_{u=1}^4 y_{111,u} + N - x_0 - \sum_{u=1}^4 y_{000,u} + 0.5$, $d_5 = y_{111,1} + y_{110,1} + y_{011,1} + y_{100,1} + y_{101,1} + y_{010,1} + y_{001,1} + y_{000,1} + 0.5$, and $w_l = \log[1 + \exp(-b_l)]$. The full conditional distribution of the

parameter of interest N is given by

$$\begin{aligned}\pi(N|\boldsymbol{\theta}_{-N}, \mathbf{x}, \mathbf{y}_{-y_{000,5}}, \mathbf{b}) &\propto \frac{(N-1)!}{(N-x_0-\sum_{u=1}^4 y_{000,u})!} [\alpha_4(1-\mathcal{P}_1)]^{N-x_0-\sum_{u=1}^4 y_{000,u}}, \\ i.e. \quad \pi(y_{000,5}|\boldsymbol{\theta}_{-N}, \mathbf{x}, \mathbf{y}_{-y_{000,5}}, \mathbf{b}) &\propto NB\left(x_0 + \sum_{u=1}^4 y_{000,u}, 1 - \alpha_4(1-\mathcal{P}_1)\right),\end{aligned}\quad (7)$$

where $y_{000,5} = N - x_0 - \sum_{u=1}^4 y_{000,u}$, and NB denotes for negative binomial distribution. The detailed derivations of the full conditional distributions are provided in the Appendix C.3-C.5. Now, one can easily execute the algorithm provided in Section 3.2 to generate sample from the posterior distribution $\boldsymbol{\theta}$ using Gibbs sampling. A summary statistics of the posterior distribution can be used to find a point estimate of N based on a suitable choice of loss function. We refer these estimates as THBM-I.

Prior Choice II

Here, we consider informative priors on $\boldsymbol{\alpha}$ and $\boldsymbol{\delta}$, and the Jeffrey's prior for the parameter of interest N is considered as before. Based on the subjective choices of the hyperparameters, we propose Dirichlet prior for $\boldsymbol{\alpha}$ with parameter vector $(\beta_1, \beta_2, \beta_3, \beta_4, \beta_5)$, and gamma prior for δ_l with scale λ_l and shape γ_l , for $l = 1, 2, 3$. Here also, the full conditional distributions of $\boldsymbol{\alpha}$ and δ_l posses closed form expressions and are given by

$$\begin{aligned}\pi(\boldsymbol{\alpha}|\boldsymbol{\theta}_{-\alpha}, \mathbf{x}, \mathbf{y}, \mathbf{b}) &\propto \text{Dirichlet}(\mathbf{d}^*), \\ \pi(\delta_l|\boldsymbol{\theta}_{-\delta_l}, \mathbf{x}, \mathbf{y}, \mathbf{b}) &\propto \text{Gamma}\left(\gamma_l + 1, \left(w_l + \frac{1}{\lambda_l}\right)^{-1}\right), \quad l = 1, 2, 3,\end{aligned}$$

where $\mathbf{d}^* = (d_1^*, d_2^*, d_3^*, d_4^*, d_5^*)$ with $d_u^* = d_u - 0.5 + \beta_u$ for $u = 1, 2, \dots, 5$. The derivations of the full conditional distributions are provided in the Appendix C.3-C.5. In order to consider diffuse prior on δ_l , one can choose the hyperparameters γ_l and λ_l appropriately such that variance of the prior distributions are large. The conditional posterior distribution of N remains the same as provided in (7). Here also, the full conditionals are from standard family of distributions and one can use Gibbs sampler for inferential purpose and we refer the associated estimates as THBM-II.

4 Simulation Study

In this section, we compare the performance of the proposed estimators with the relevant competitors based on the following models - log-linear model (LLM) (Fienberg, 1972b), M_{tb} model (Chao et al., 2000; Chatterjee and Bhuyan, 2020a), quasi-symmetry model (QSM) (Darroch et al., 1993), partial quasi-symmetry model (PQSM) (Darroch et al., 1993), non-parametric sample coverage method (SC) (Chao and Tsay, 1998) and independent model i.e. LLM without interaction effects (Independent) (Fienberg, 1972b) through an extensive simulation study. The details of these existing models and associated estimates are briefly presented in Appendix B. We consider six different choices of α representing varying degree of list dependence and denote them as P1-P6 in Table 1. We generate TRS data from the proposed model keeping total population size N fixed at 200 and 500 for each of these six different choices of populations P1-P6 with five different combinations of random-effects characterized by δ given as $\{(1.6, 1.2, 0.8), (1.3, 1.7, 0.9), (1.0, 1.4, 1.8), (0.8, 0.8, 0.8), (1.6, 1.6, 1.6)\}$. Note that $\delta = (0.8, 0.8, 0.8)$ and $(1.6, 1.6, 1.6)$ present the cases where capture probabilities of the causally independent individuals in all the three lists are identically distributed. In contrast, the capture probabilities differ from one list to another for the other three choices of δ .

Table 1: Dependence structure of the simulated populations.

Population	$(\alpha_1, \alpha_2, \alpha_3, \alpha_4)$	$1 - \alpha_0$
P1	(0.35, 0.15, 0.25, 0.10)	0.15
P2	(0.30, 0.30, 0.15, 0.10)	0.15
P3	(0.20, 0.10, 0.20, 0.10)	0.40
P4	(0.10, 0.20, 0.30, 0.20)	0.20
P5	(0.20, 0.20, 0.20, 0.20)	0.20
P6	(0.25, 0.15, 0.35, 0.10)	0.10

We consider two different sets of prior as discussed in the Subsection 3.2.1 for estimation of the proposed model. Jeffrey's priors (Prior Choice I) are considered in THBM-I, and for THBM-II, we consider $\beta_i = 8\alpha_i$ for $i = 1, 2, \dots, 5$, and diffuse prior for δ_l using gamma distribution with mean δ_l and variance 100, for $l = 1, 2, 3$ (Prior Choice II). We generate 50,000

samples from the posterior distributions of the parameters associated with THBM using Gibbs sampling and find the posterior median of the population size based on every 10th iterate discarding the first 25,000 iterations as burn-in. This is repeated 1000 times and the average estimate \hat{N} are reported in Tables D.1-D.6 provided in the Appendix D. We also report the 95% highest posterior density (HPD) credible interval along with coverage probability (CP) of N and the Relative Mean Absolute Error, defined as $RMAE = \frac{1}{1000} \sum_{r=1}^{1000} \left| \frac{\hat{N}_r - N}{N} \right|$, where \hat{N}_r denotes the estimate based on data generated at the r th replication. Similarly, we compute the RMAE of all the existing competitors. For each of these 1000 replications, 95% confidence interval (CI) of N for these competitive methods are obtained based on the quantiles from 1000 bootstrap samples. The CP of the population size N is also obtained based on the bootstrap CIs.

The proposed model performs the best in terms of RAME for all the simulated populations P1-P6 for both $N = 200$ and $N = 500$. Moreover, the CPs of the proposed estimates are higher than all the existing competitors except M_{tb} model which possesses a very wide CI due to high variability. In most of the cases, the CP of QSM and PQSM estimates are comparable for $N = 200$ but CP of PQSM estimate is lower than QSM estimate for $N = 500$. The CP of LLM estimate is lower than PQSM estimates for both $N = 200$ and $N = 500$. It is important to note that the CIs associated with the independent model and the SC estimates are very tight and that results in extremely low CPs. In particular, the CPs of the SC estimates are less than 6% for P4 and P5 (See Appendix D, Tables D.4-D.5), and the highest is around 55% attained for only two cases in P3 with $N = 200$ (See Appendix D, Table D.3). Also, the independent model and SC method consistently underestimate N for all populations P1-P6. Interestingly, the M_{tb} model underestimates for P4 and P5 and overestimates for the rest of the populations. It is also observed that the RAME of all the estimators except the independent model and SC method decreases as N increases from 200 to 500 for all simulated population P1-P6.

As discussed in Appendix B.4, we have observed that the SC estimate suffers from boundary problems in our simulation study. It is easy to generate data such that the percentage of infeasible estimates is as high as 60% to 80%. In some other cases, we have also observed that the QSM, PQSM, and LLM may fail to converge and produce extremely large estimates. For a valid and fair comparison, we have not reported those cases here.

4.1 Sensitivity Analysis

4.1.1 Sensitivity of Prior Specification

As discussed before, the proposed estimates of the population size N based on two different sets of priors perform better than the existing competitors. But to understand the sensitivity of the estimate with prior specifications, we now compare the results associated with THBM-I and THBM-II in Tables D.1-D.6 (See Appendix D). In general, the CPs of the estimates of N with both the prior specifications are very similar, but only in few cases, CPs of THBM-I are marginally lower than those of THBM-II. Although the performance of the THBM-II is better than THBM-I for all the simulated populations P1-P6 in terms of RMAE, the difference is merely less than 3%. The marginal improvement is due to the fact that the prior variance of α_i 's considered in THBM-II are considerably smaller compared to the variance of Jeffer's prior in THBM-I. From these observations, it indicates that the proposed methodology is not sensitive to prior specifications, and these are especially valuable when only limited prior information is available.

4.1.2 Sensitivity of Random Effects

In the posed estimation methodology, we are obliged to assume that the random effects b_l 's follow generalized logistic distribution to obtain a closed form expression of the full conditionals. However, this assumption may not be valid in real applications and it is worth investigating the effect of misspecification of random effects distributions on the performance of the proposed estimate. For this purpose, we generate data for populations P1-P6 considering random effects from generalized logistic type-I (GL_I), normal and, gamma distributions with two different parameter choices provided in Table 2. The RAMEs and CPs of THBM-I are plotted in Figure 1 and Figure 2, respectively. In terms of RAME, we observe minor deterioration due to misspecification when the true random effects are generated from gamma distributions, but in contrast, marginal improvement is observed when random effects are generated from the normal distributions. In all the six populations P1-P6, the range of differences in RAMEs is only less than 3% (See Figure 1). However, no effect of misspecification is noticed on CPs in any of the six populations (See Figure 2). We observed similar results for THBM-II (not reported here).

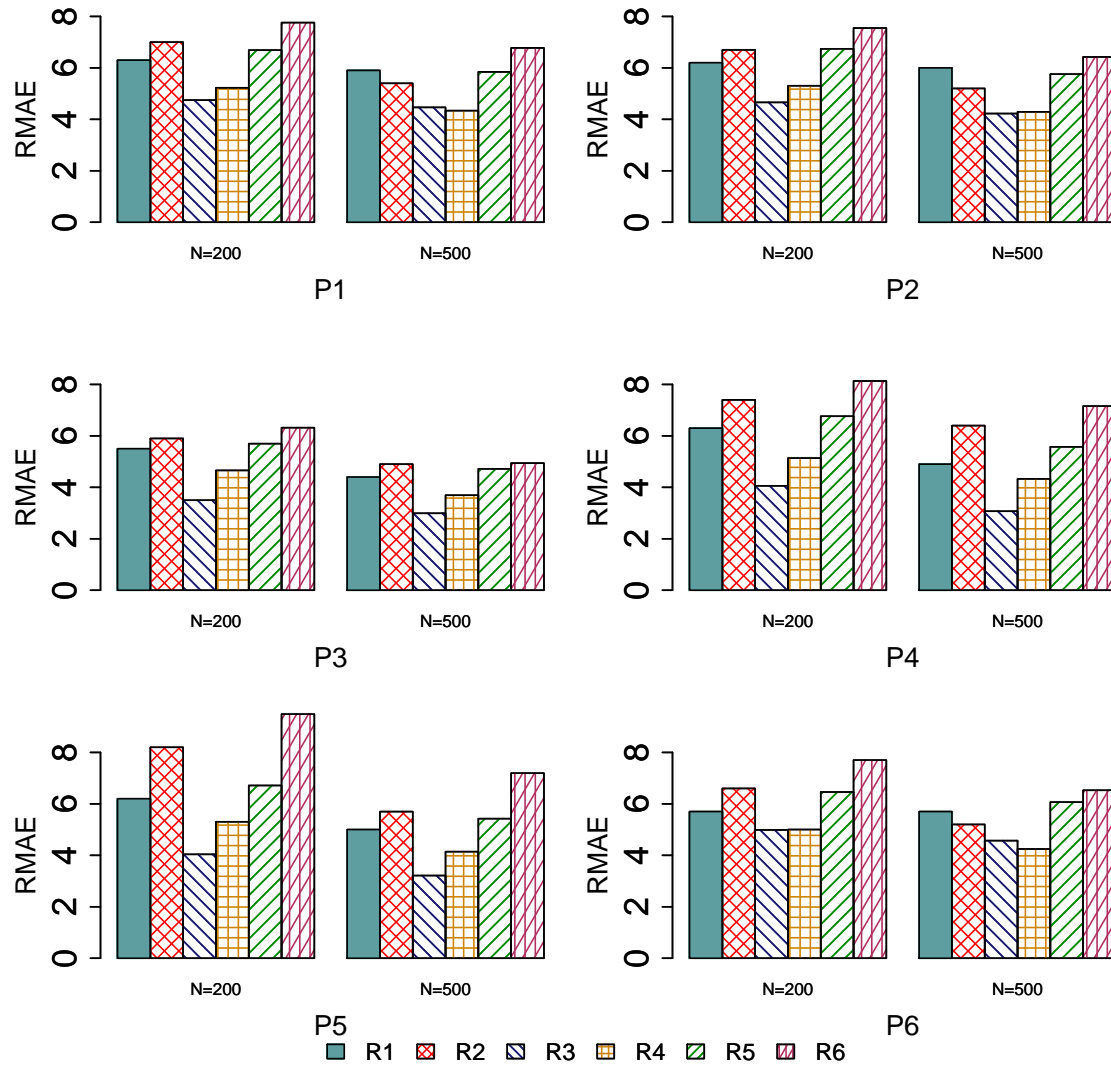


Figure 1: Comparison of RAMEs (in %) of the proposed estimate under different random effects models for data generation.

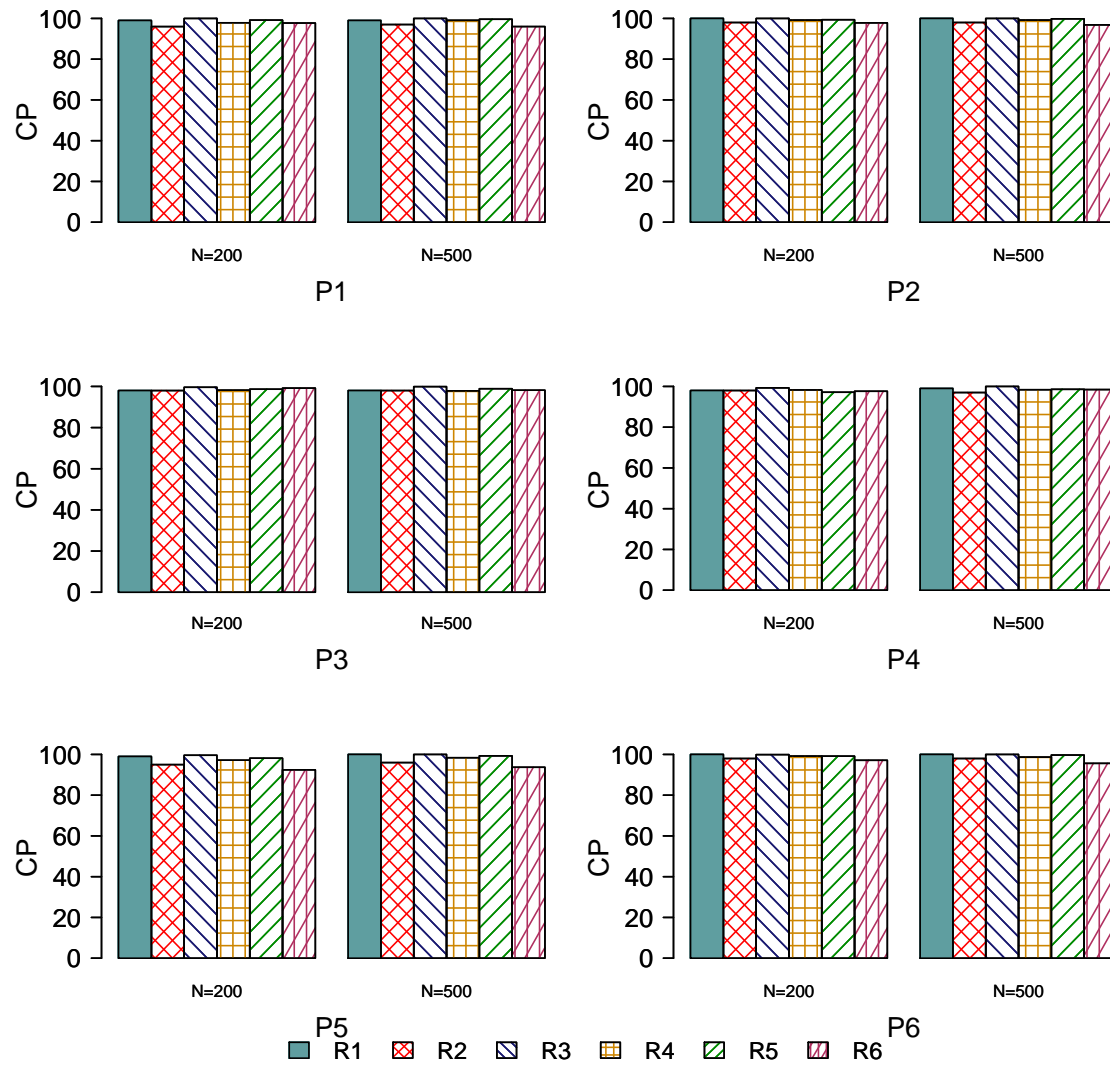


Figure 2: Comparison of coverage probabilities (in %) of the proposed estimate under different random effects models for data generation.

Table 2: Random effects distributions for analysing sensitivity of misspecification.

Random Effects	b_1	b_2	b_3
R1	$GL_I(1.6)$	$GL_I(1.6)$	$GL_I(1.6)$
R2	$GL_I(1.6)$	$GL_I(1.2)$	$GL_I(0.8)$
R3	$Normal(0.5, 1)$	$Normal(0.5, 1)$	$Normal(0.5, 1)$
R4	$Normal(0.5, 1)$	$Normal(0, 1)$	$Normal(-0.5, 1)$
R5	$Gamma(2, 0.5)$	$Gamma(2, 0.5)$	$Gamma(2, 0.5)$
R6	$Gamma(2, 0.5)$	$Gamma(1, 0.5)$	$Gamma(0.5, 0.5)$

$GL_I(\eta)$ denotes generalized logistic type-I distribution with parameter η .

$Normal(\mu, \sigma)$ denotes normal distribution with mean μ and standard deviation σ .

$Gamma(a, b)$ denotes gamma distribution with shape parameter a and scale parameter b .

4.1.3 Sensitivity of Model Misspecification

As discussed in Section 2, the proposed model represents a realistic mechanism to account for inherent heterogeneity among the individuals and dependencies. Nevertheless, it is important to study the effect of model misspecification when the data generating mechanism deviates from the assumed structure of the fitted model. For this purpose, we generate the capture statuses of the individuals $Z_h^{(1)}, Z_h^{(2)}, Z_h^{(3)}$ from Bernoulli distributions with respective probabilities $P_h^{(1)}, P_h^{(2)},$ and $P_h^{(3)}$, where $P_h^{(j)} = \min\{P_h^{(j-1)}\mathbb{I}[Z_h^{(j-1)} = 0] + 1.2\mathbb{I}[Z_h^{(j-1)} = 1], 0.99\}$, for $j = 2, 3$, and $h = 1, \dots, N$. This mechanism induces a dependence structure among the capture statuses similar to a first-order auto-regressive model. To incorporate heterogeneity in the capture probabilities, we generate $P_h^{(1)}$'s from three different choices of distributions: (i) $Uniform(0, 1)$, (ii) $Beta(4, 2)$, and (iii) $Beta(2, 2)$. The RAMEs and CPs of THBM-I and its competitors are plotted in Figure 3 and Figure 4, respectively. Here also, the proposed estimator outperforms the existing competitors with respect to RAME as discussed in Section 4. The CPs of the proposed estimator and M_{tb} model are close to 100% and much better than all other estimators. In particular, the performance of SC is very poor and its CPs are less than 40% in all the cases.

5 Case Study

As discussed before, applications of MSE are commonly found in the domain of epidemiology. In this section, we consider two different case studies on infectious diseases. The results from

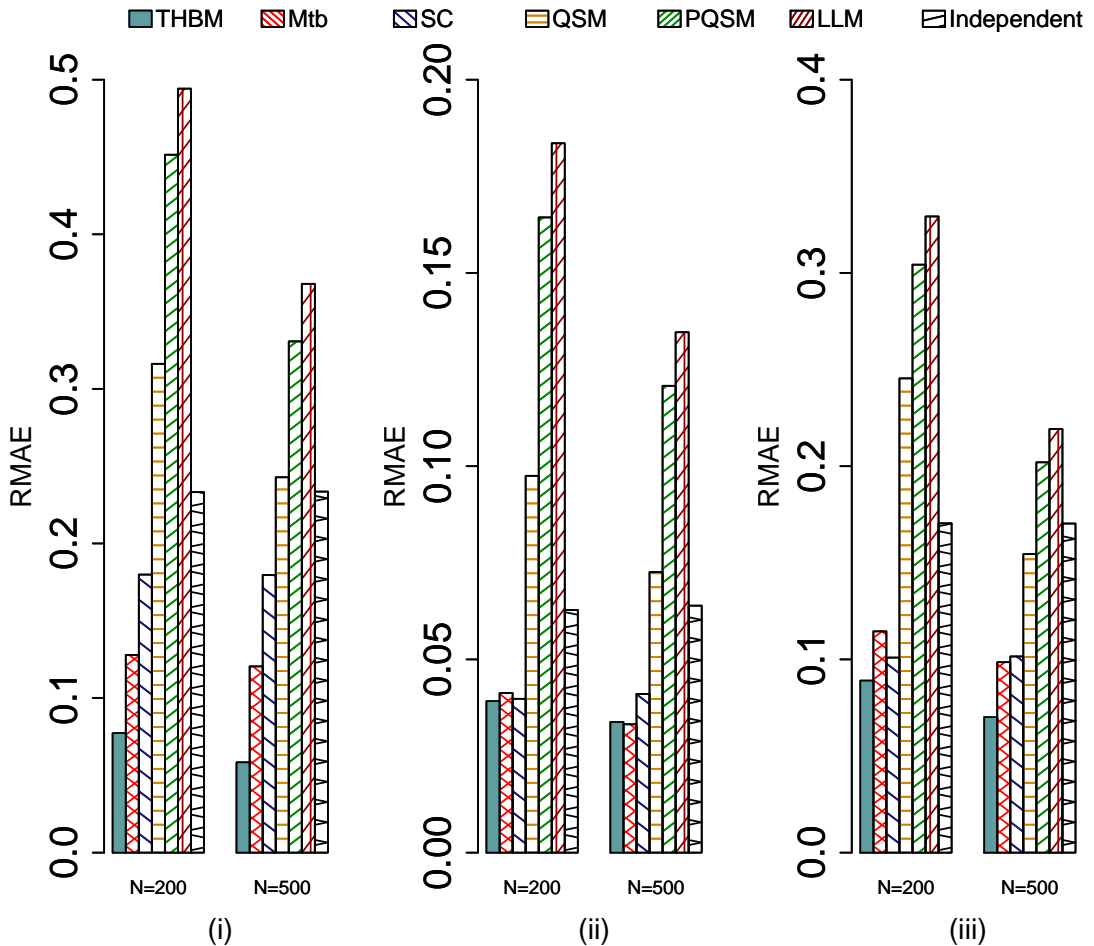


Figure 3: Comparison of the proposed estimate with the existing competitors under model misspecification with respect to RAME (in %) when data generated from auto-regressive dependence structure with capture probabilities $P_h^{(1)}$'s in the list L_1 follow (i) $Uniform(0, 1)$, (ii) $Beta(4, 2)$, and (ii) $Beta(2, 2)$.

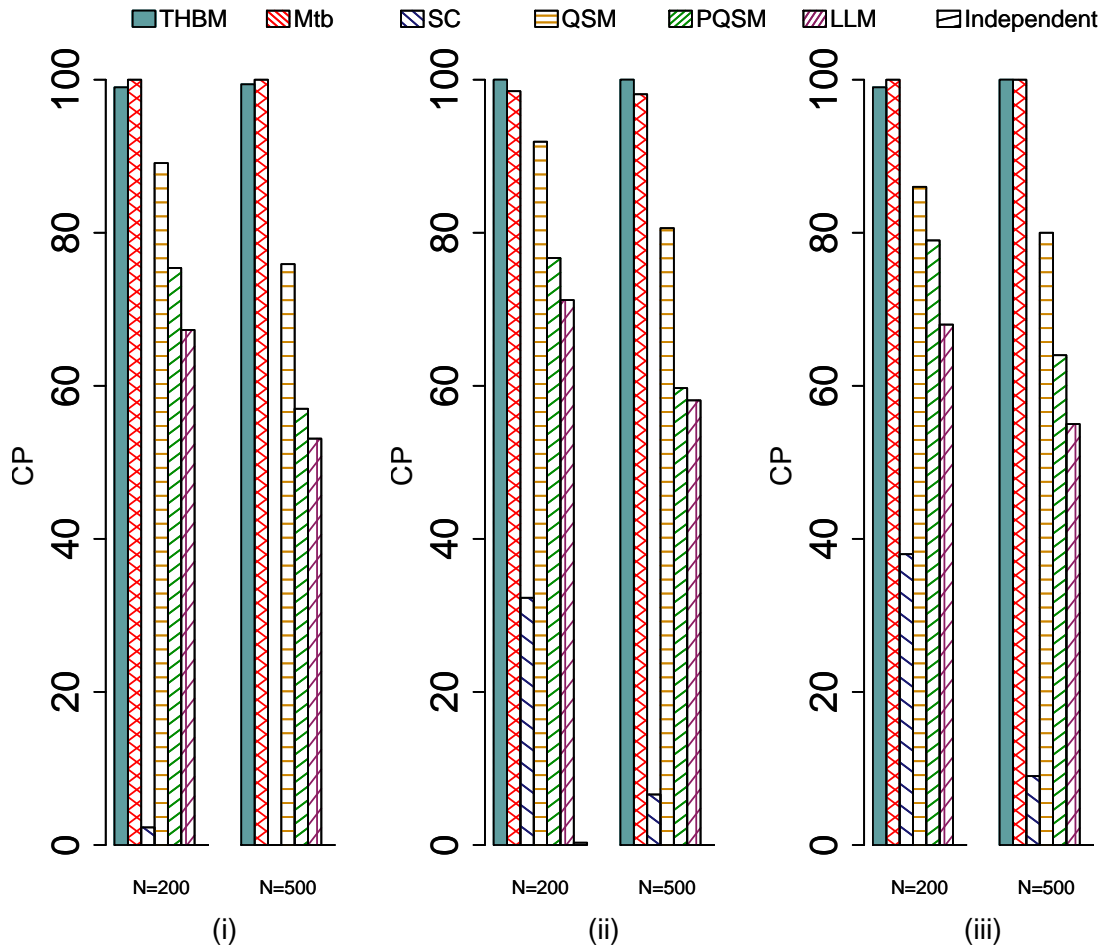


Figure 4: Comparison of the proposed estimate with the existing competitors under model misspecification with respect to CP (in %) when data generated from auto-regressive dependence structure with capture probabilities $P_h^{(1)}$'s in the list L_1 follow (i) $Uniform(0, 1)$, (ii) $Beta(4, 2)$, and (iii) $Beta(2, 2)$.

analyses of the two datasets based on the proposed methodology are discussed below along with the practical implications. We also compare these results with the estimates based on the existing methods.

5.1 Analysis of Legionnaires' Disease Surveillance Data

As discussed in Section 1, we consider a dataset on the LD outbreak in the Netherlands in the year 1999. To apply the proposed methodology to estimate the total number of infected individuals, we consider Jeffrey's prior for all the parameters as discussed in Subsection 3.2.1. We generate 1 million samples from the posterior distributions of the associated model parameters using the Gibbs sampling algorithm and discard the first 10% iterations as burn-in. The convergence of the chains is monitored graphically and using Geweke's diagnostic test. The median, MAE, and the 95% HPD credible interval of N are reported in Table 3. We also report the estimates of N based on different existing methods. The estimated MAE and CI are computed based on 10,000 bootstrap samples. The estimates based on the independent model and SC method are considerably lower than other estimates. The results based on the proposed method and PQSM are comparable. The largest estimate results from QSM with relatively larger MAE and the estimates based on LLM and M_{tb} are larger than that of PQSM.

To gain insight from our analysis, we present the posterior density of N and boxplot of the capture probabilities associated with DNR, Laboratory and Hospital records in Figure 5(a), and Figure 5(b), respectively. The posterior density of N is slightly skewed toward the right and the catchability of Hospital records is considerably higher than those of DNR and Laboratory records. It is also seen that the heterogeneity in capture probability associated with Hospital records is higher compared to other sources. From Figures 5(c)-5(f), it is visible that the bulk of the distribution of all the dependence parameters is away from 0 which indicates their significance. The estimates of the dependence parameters suggest that almost 60% individuals are causally dependent, and 13% of individuals have perfect positive association among the three lists.

To reduce the extent of heterogeneity as well as the dependence that is induced by heterogeneity in the population, it is often recommended to employ post-stratification of the population based on appropriate demographic (e.g. age, race or sex) or geographic variables (Wolter, 1986; Islam, 2015). In this application, we also estimate the prevalence of LD in four regions:

North (1,671,534 inhabitants), East (4,467,527 inhabitants), West (5,955,299 inhabitants) and South (3,892,715 inhabitants) to facilitate regional surveillance and identification of associated risk factors. The results based on the proposed method are presented in Table 4. It is quite common to observe that the sum of the strata-wise estimate of the population sizes does not tally with the estimate obtained from the combined data if the underlining heterogeneity is not successfully accounted for. In this context of capture-recapture experiments, this phenomenon is popularly known as Simpson's paradox or simply Yule's association paradox (Kadane et al., 1999). Interestingly, the estimate of the total LD incidence obtained by summing the four regional estimates approximately matches with the national estimate based on combined data (See Tables 3-4). It is an indication that the proposed method successfully accounted for the heterogeneity present in the population. Additionally, we report the under-reporting rate (UR) and incidence rate (IR)¹ for each of these four regions based on our estimate of the prevalence. The estimated UR in the North and West are similar but marginally lower than that in the South. However, the estimated UR in the East is significantly higher than in other regions. We also observe that the CI associated with the estimate of LD incidence in the East is wide, and the corresponding MAE is also very high. This encourages further investigation, possibly involving information from other sources, to obtain a more reliable estimate. As mentioned before, the capture probability associated with Laboratory records is very low (See Figure 5(b)), and it is worth considering alternative sources with higher capture probability to improve the coverage. The IR is the highest in the South and least in the North. However, a marginal difference in IR is observed between East and West. Some previous studies suggest that weather and climatic conditions are associated with LD incidence (Karagiannis et al., 2009; Brandsema et al., 2014). On average, the northern provinces endure lower temperatures compared to the southern provinces. In particular, the east of Brabant and the very north of Limburg are the warmest during summer. Our analyses indicate that warm weather increases LD incidence, which supports the findings by Karagiannis et al. (2009) and Brandsema et al. (2014). Recently, researchers are also interested in the association between LD incidence and precipitation and humidity (Passer et al., 2020). In general, there is no dry season in the Netherlands, and precipitation is common throughout the year. This is perhaps one of the major risk factors causing a higher IR in the Netherlands compared to other countries. In

¹UR = $\frac{(\hat{N} - x_0)}{\hat{N}} \times 100$, IR = $\frac{\hat{N}}{\text{No. of inhabitants}} \times 100,000$

particular, the coastal provinces (West) experience the heaviest rain showers after the summer and during the autumn results in higher IR compared to the North. Several other factors related to demographics and socioeconomic characteristics may lead to higher incidence of LD ([Farnham et al., 2014](#); [Passer et al., 2020](#)). Following a similar post-stratification strategy, as considered in this article, one can effectively support the general goals of surveillance. It helps to rapidly recognize cases that occur in similar locations and describe incidence and trends. Also, one can identify opportunities for prevention and monitor the effectiveness of interventions implemented as part of an outbreak investigation ([Centers for Disease Control and Prevention, 2021](#)).

Table 3: Summary results of the Legionnaire’s disease surveillance data analysis.

	THBM	SC	QSM	PQSM	LLM	M_{tb}	Independent
\hat{N}	1114	992	1803	1176	1253	1400	855
MAE	85	32	225	85	123	124	10
CI*	(940, 1335)	(922, 1078)	(1387, 2509)	(923, 1363)	(986, 1614)	(1153, 2104)	(829, 878)

THBM: Trivariate Heterogeneous Bernoulli Model; SC: Sample Coverage; QSM: Quasi-symmetry Model; PQSM: Partial Quasi-symmetry Model; LLM: Log-linear Model, M_{tb} : Time Behavioural Response Variation Model; Independent: LLM without interaction effects.

* HPD Credible Interval for THBM

Table 4: Summary results of the region wise Legionnaire’s disease surveillance data analysis based on THBM.

	North	South	East	West
\hat{N}	95	308	318	387
MAE	21	30	105	38
CI*	(70, 168)	(259, 401)	(216, 685)	(317, 492)
IR	5.7	7.9	7.1	6.5
UR	27	32	42	26

IR: Incidence rate per 100000 inhabitants; UR: Underreporting rate in %

* HPD Credible Interval for THBM

5.2 Analysis of Hepatitis A Virus Surveillance Data

Here, we consider the surveillance data of the HAV outbreak in northern Taiwan in the year 1995 to estimate the total number of infected individuals. For this purpose, we generate 5

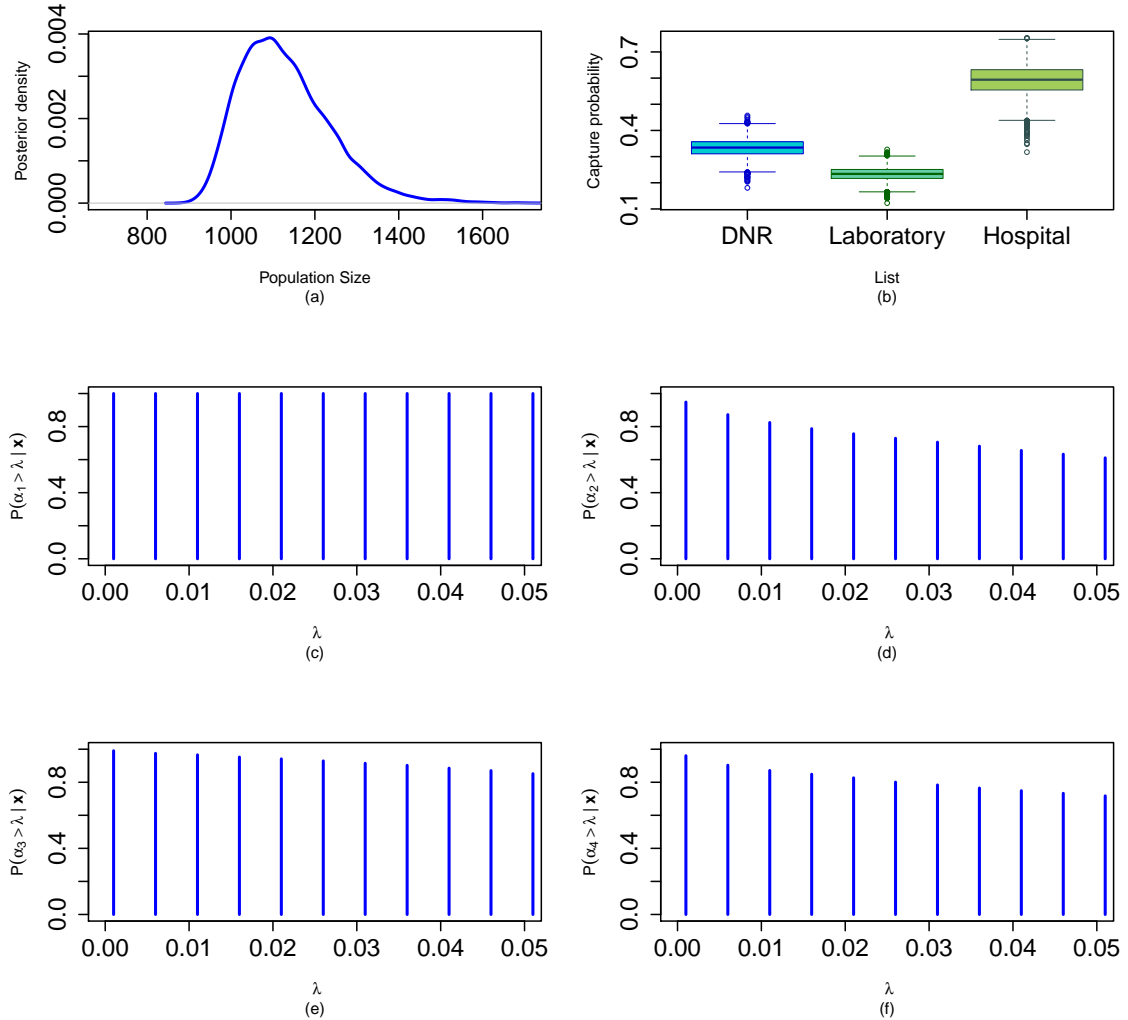


Figure 5: (a) Posterior density of the size of population affected with Legionnaires' disease; (b) Boxplots of capture probabilities associated with three different lists; (c) Test of significance of α_1 ; (d) Test of significance of α_2 ; (e) Test of significance of α_3 ; (f) Test of significance of α_4 .

million samples using the Gibbs sampling from the posterior distributions of the associated model parameters and discard the first 20% iterations as burn-in. Here also, no convergence issues are found based on Geweke's diagnostic test. The estimates of N along with MAE and 95% HPD credible interval are reported in Table 5. We also provide the results based on the existing methods for comparison. Here also, the estimate based on the independent model is considerably lower than other estimates. The proposed estimate is marginally larger than that of M_{tb} but considerably lower than that of LLM. The estimates based on QSM, PQSM, and LLM are comparable but the CI of both QSM and PQSM is wider than that of LLM. The estimated sample coverage $\hat{C} = 51\%$ indicates the estimates provided by the SC method are not reliable.

From Figure 6(a), one can observe that the posterior distribution of N is highly skewed. The catchability of all three lists is similar but the heterogeneity in capture probability associated with P-list (i.e. records based on a serum test) is marginally higher than that of the other lists (See Figure 6(b)). Cases of HAV are not clinically distinguishable from other types of acute viral hepatitis, which results in low capture probability in all the sources ([World Health Organization, 2021](#)). Here also, the bulk of the distribution of all the dependence parameters is significantly away from 0 (See Figure 6(c)-6(f)). Almost 29% individuals are causally dependent, and 15% of individuals have perfect positive association among the three lists.

In December 1995, the National Quarantine Service of Taiwan conducted a screen serum test for the HAV antibody for all students at the college at which the outbreak of the HAV occurred to determine the number of infected students. Based on their final figure, the estimated UR is 50% ([Chao et al., 1997](#)), but our estimate of the UR is 57%. Nevertheless, the level of underreporting of HAV cases are considerably high. As effective interventions to control further spread of HAV are available, underreporting leads to serious consequences because it prevents prompt and effective public health action to protect immediate contacts of cases and their communities ([Crowcroft et al., 2001](#)). After this outbreak, Taiwan started to immunize children in 30 indigenous townships against HAV and further expanded to 19 non-indigenous townships with higher incidence or increased risk of epidemic in 1997-2002. It has been reported that the annual IR of HAV decreased from 2.96 in 1995 to 0.90 in 2003-2008. The IR in vaccinated townships and unvaccinated townships declined 98.3% and 52.6%, respectively ([Tsou et al., 2011](#)). This apparently indicates the long-term efficacy of the HAV vaccine in

disease control in the vaccinated population and the out-of-cohort effect in the unvaccinated population. However, these figures do not account for the underreported cases, and any conclusion drawn from these statistics may be misleading. In particular, vaccination efficacy is overestimated when UR is higher in the vaccinated population compared to the unvaccinated population. Therefore, it is essential to estimate the underreported cases and adjust the calculation of IR (as considered in Subsection 5.1) for an unbiased evaluation of the interventions. For this purpose, the proposed model is a good choice to obtain an efficient estimate of the total number of individuals (or equivalently the underreported cases) infected by a disease such as HAV.

In 2003-2008, IR doubled in unvaccinated townships among those aged more than 30 years (Tsou et al., 2011). The lack of demographic or geographical information for this case study hampered our ability to carry out a stratified analysis. At the national level, geographical analysis of outbreaks can support surveillance and identification of associated risk factors. Without detailed risk factor information, it is difficult to develop and implement appropriate policies to contain the spread of this infection (Matin et al., 2006).

Table 5: Summary results of the HAV surveillance data analysis.

	THBM	SC	QSM	PQSM	LLM	M_{tb}	Independent
\hat{N}	633	971	1313	1325	1312	587	388
MAE	203	1415	457	387	279	146	25
CI	(400, 1472)	(557, 3583)	(669, 3171)	(607, 2718)	(464, 1961)	(287, 1110)	(381, 510)

THBM: Trivariate Heterogeneous Bernoulli Model; SC: Sample Coverage; QSM: Quasi-symmetry Model; PQSM: Partial Quasi-symmetry Model;

LLM: Log-linear Model, M_{tb} : Time Behavioural Response Variation Model; Independent: LLM without interaction effects.

* HPD Credible Interval for THBM

6 Discussions

In this paper, the issue of population size estimation incorporating the possible list dependence arising from both behavioural response variation and heterogeneous catchability has been addressed. For this purpose, a novel model for capture-recapture data is considered and a Bayesian methodology has been developed to estimates the population size based on data augmentation. In particular, the Gibbs sampling method has been developed to make the computation fast and implementation easy for the practitioners. The proposed method seems to

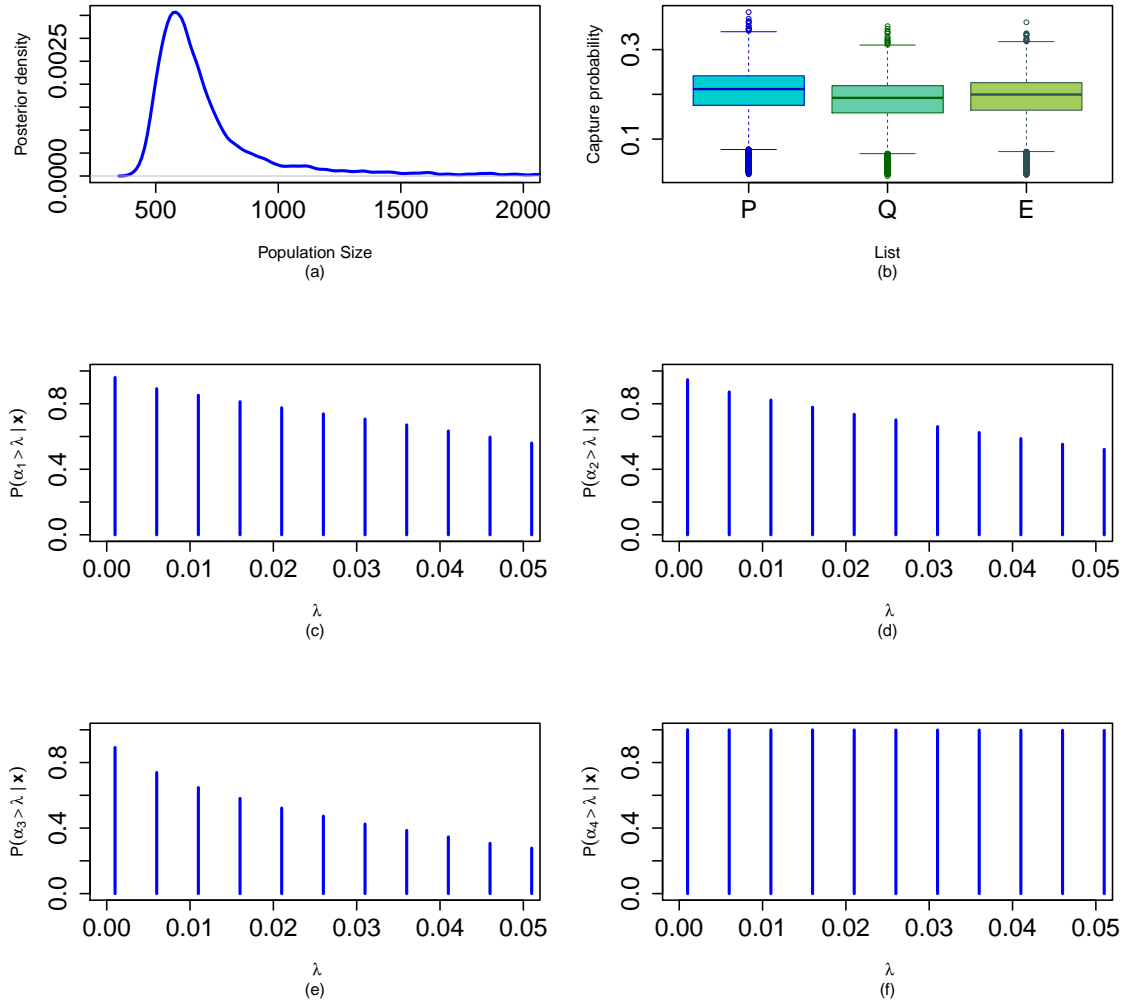


Figure 6: (a) Posterior density of the size of HAV infected population; (b) Box plots of capture probabilities associated with three different lists; (c) Test of significance of α_1 ; (d) Test of significance of α_2 ; (e) Test of significance of α_3 ; (f) Test of significance of α_4 .

have an edge in terms of ease of interpretation and to have a much wider domain of applicability in the fields of public health, demography, and social sciences. From the simulation study, we can see that the proposed method exhibit a remarkable improvement over the existing models. Moreover, the proposed method is robust with respect to model misspecification. Along with the estimate of the population size, the posterior distribution of the associated dependence parameters and capture probabilities provide specific insights into the capture–recapture mechanism. In particular, the proposed method provides a clear picture of the nature and the extent of behavioral dependence of the individuals in the population under consideration. In real applications, we exhibit the importance of geospatial analysis of outbreaks in surveillance and identification of associated risk factors. We also emphasized the necessity to adjust the conventional method of calculating IR incorporating the estimated size of the underreported cases for an unbiased evaluation of the interventions. In a frequentist setup, a possible direction for further research could be the development of an estimation methodology based on a suitable pseudo likelihood approach. Multiple systems estimation strategies have recently been applied to estimate the number of victims of human trafficking and modern slavery. In this context, it is not uncommon to find sparse or even no overlap between some of the lists on which the estimates are based ([Chan et al., 2020](#)). It will be an interesting problem to model such data by using the TBM and to develop an associated estimation methodology.

Acknowledgement

The authors are grateful to Prof. Brian W. Junker for providing R programs related to Rasch models. The authors also like to thank Mr. Debjit Majumder for his help in creating the bar diagrams. The work of Dr. Prajamitra Bhuyan is supported in part by the Lloyd’s Register Foundation programme on data-centric engineering at the Alan Turing Institute, UK. The work of Dr. Kiranmoy Chatterjee is supported by the Core Research Grant (CRG/2019/003204) on Mathematical Sciences by the Science and Engineering Research Board, Department of Science & Technology, Government of India.

References

Aldrich, J. (2002). How likelihood and identification went bayesian. *International Statistical Review*, 50:1–25. [10](#)

Bird, S. M. and King, R. (2018). Multiple systems estimation (or capture-recapture estimation) to inform public policy. *Annu Rev Stat Appl.*, 5:95–118. [1](#), [2](#)

Bishop, Y. M. M., Fienberg, S. E., and Holland, P. W. (1975). *Discrete multivariate analysis: Theory and practice*. Cambridge, MA: The MIT Press. [2](#)

Bohning, D. and Heijden, P. V. D. (2009). Recent developments in life and social science applications of capture–recapture methods. *Advanced Statistical Analysis*, 93:1–3. [2](#)

Brandsema, P. S., Euser, S. M., Karagiannis, I., Den Boer, J. W., and Van Der Hoek, W. (2014). Summer increase of legionnaires’ disease 2010 in the netherlands associated with weather conditions and implications for source finding. *Epidemiology and Infection*, 142(11):2360–2371. [24](#)

Brown, C. R., MacLachlan, J. H., and Benjamin, C. C. (2017). Addressing the increasing global burden of viral hepatitis. *Hepatobiliary Surgery and Nutrition*, 6(4):274–276. [4](#)

Centers for Disease Control and Prevention (2021). CDC surveillance classifications. <https://www.cdc.gov/legionella/health-depts/surve-reporting/surveillance-classifications.html>. [25](#)

Chan, L., Silverman, B. W., and Vincent, K. (2020). Multiple systems estimation for sparse capture data: Inferential challenges when there are non overlapping lists. *Journal of the American Statistical Association*. [30](#)

ChandraSekar, C. and Deming, W. E. (1949). On a method of estimating birth and death rates and the extent of registration. *Journal of the American Statistical Association*, 44:101–115. [2](#)

Chao, A. (2001). An overview of closed capture–recapture models. *Journal of Agricultural, Biological, and Environmental Statistics*, 6:158–175. [5](#)

Chao, A., Chu, W., and Chiu, H. H. (2000). Capture-recapture when time and behavioral response affect capture probabilities. *Biometrics*, 56:427–433. [15](#), [3](#)

Chao, A., Lee, S. M., and Jeng, S. L. (1992). Estimating population size for capture-recapture data when capture probabilities vary by time and individual animal. *Biometrics*, 48:201–216. [5](#)

Chao, A. and Tsay, P. K. (1998). A sample coverage approach to multiple-system estimation with application to census undercount. *Journal of American Statistical Association*, 93:283–293. [5](#), [8](#), [10](#), [15](#)

Chao, A., Tsay, P. K., Lin, S. H., Shau, W. Y., and Chao, D. Y. (2001). The application of capture-recapture models to epidemiological data. *Statistics in Medicine*, 20:3123–3157. [2](#), [5](#), [10](#), [3](#)

Chao, D., Shau, W., Lu, C., Chen, K., Chu, C., Shu, H., and Horng, C. (1997). A large outbreak of hepatitis A in a college school in Taiwan: associated with contaminated food and water dissemination. *Epidemiology Bulletin, Department of Health, Executive Yuan, Taiwan Government*, page 693–702. [4](#), [27](#)

Chatterjee, K. and Bhuyan, P. (2020a). On the estimation of population size from a dependent triple-record system. *Journal of Royal Statistical Society, Series A*, 182:1487–1501. [5](#), [6](#), [8](#), [10](#), [15](#), [3](#)

Chatterjee, K. and Bhuyan, P. (2020b). On the estimation of population size from a post-stratified two-sample capture–recapture data under dependence. *Journal of Statistical Computation and Simulation*, 819–838. [2](#)

Chatterjee, K. and Mukherjee, D. (2016). On the estimation of homogeneous population size from a complex dual-record system. *Journal of Statistical Computation and Simulation*, 86:3562–3581. [2](#)

Chen, W. C., Chiang, P. H., Liao, Y. H., Huang, L. C., Hsieh, Y. J., Chiu, C. M., Lo, Y. C., Yang, C. H., and Yang, J. Y. (2019). Outbreak of hepatitis A virus infection in Taiwan, June 2015 to September 2017. *Euro Surveill*, Apr 4:24(14). [4](#)

Cormack, R. M. (1989). Log-linear models for capture-recapture. *Biometrics*, 45:395–413. 5

Coull, B. A. and Agresti, A. (1999). The use of mixed logit models to reflect heterogeneity in capture-recapture studies. *Biometrics*, 55:294–301. 9

Coumans, A. M., Cruyff, M., Heijden, P. G. M., Heijden, V. D., Wolf, J., and Schmeets, H. (2017). Estimating homelessness in the Netherlands using a capture-recapture approach. *Social Indicators Research*, 130:189–212. 5

Crowcroft, N., Walsh, B., Davison, K. L., Gungabissoon, U., and PHLS Advisory Committee on Vaccination and Immunisation (2001). Guidelines for the control of hepatitis a virus infection. *Communicable Disease and Public Health*, 4(3):213–227. 27

Cruyff, M., Van Dijk, J., and van der Heijden, P. G. M. (2017). The challenge of counting victims of human trafficking: Not on the record: A multiple systems estimation of the numbers of human trafficking victims in the Netherlands in 2010–2015 by year, age, gender, and type of exploitation. *Chance*, 30:41–49. 2

Cuthbert, J. A. (2001). Hepatitis A: old and new. *Clin Microbiol Rev*, 14:38–58. 4

Darroch, J. N. (1981). The Mantel-Haenszel test and tests of marginal symmetry: Fixed-effects and mixed models for a categorical response. *International Statistical Review*, 49:285–307. 4

Darroch, J. N., Fienberg, S. E., Glonek, G. F. V., and Junker, B. W. (1993). A three-sample multiple-recapture approach to census population estimation with heterogeneous catchability. *Journal of the American Statistical Association*, 88:1137–1148. 8, 15, 4, 5

Den, B. J. W., Friesema, I. H. M., and Hooi, J. D. (2002a). Reported cases of Legionella pneumonia in the Netherlands, 1987-2000 [in dutch]. *Ned Tijdschr Geneeskde*, 146:315–320. 4

Den, B. J. W., Yzerman, E. P. F., Schellekens, J., Lettinga, K. D., Boshuizen, H. C., Van Steenbergen, J. E., Bosman, A., Van den Hof, S., Van Vliet, H. A., Peeters, M. F., Van Ketel, R. J., Speelman, P., Kool, J. L., , and Van Spaendonck, M. A. E. C. V. (2002b). A large outbreak of Legionnaires' disease at a flower show, the Netherlands, 1999. *Emerg Infect Dis*, 8:37–43. 3

Dey, R. and Ashbolt, N. J. (2020). Legionella infection during and after the COVID-19 pandemic. *ACS ES&T Water*, acsestwater.0c00151. [3](#)

Farnham, A., Alleyne, L., Cimini, D., and Balter, S. (2014). Legionnaires' disease incidence and risk factors, new york, new york, usa, 2002-2011. *Emerging Infectious Diseases*, 20(11):1795–1802. [25](#)

Fienberg, S. E. (1972a). The analysis of incomplete multi-way contingency tables. *Biometrics*, 28:177–202. [2](#)

Fienberg, S. E. (1972b). The multiple recapture census for closed populations and incomplete 2^k contingency tables. *Biometrika*, 59:591–603. [5](#), [15](#), [2](#)

Fienberg, S. E., Johnson, M. S., and W., J. B. (1999). Classical multilevel and bayesian approaches to population size estimation using multiple lists. *Journal of the Royal Statistical Society. Series A*, 162(3):383–405. [4](#), [5](#)

Fischer, M. J. (2000). The folded EGB2 distribution and its application to financial return data. *Discussion Papers 32/2000*, pages Friedrich–Alexander University Erlangen–Nuremberg, Chair of Statistics and Econometrics. [12](#), [13](#)

Gallay, A., Vaillant, V., Bouvet, P., Grimont, P., and Desenclos, J. (2000). How many food-borne outbreaks of *Salmonella* infection occurred in France in 1995? Application of the capture–recapture method to three surveillance systems. *Am. J. Epidemiol.*, 152:171–177. [2](#)

Gustafson, P. (2005). On model expansion, model contraction, identifiability and prior information: Two illustrative scenarios involving mismeasured variables. *Statistical Science*, 20(1):111–140. [10](#)

Hook, E. B. and Regal, R. (1995). Capture–recapture methods in epidemiology: methods and limitations. *Epidemiol. Rev.*, 17:243–264. [2](#)

International Working Group for Disease Monitoring and Forecasting (1995). Capture–recapture and multiple-record systems estimation I: History and theoretical development. *American Journal of Epidemiology*, 142:1047–1058. [2](#)

Islam, H. W. (2015). *Estimating the Missing People in the UK 1991 Population Census*. AuthorHouse, UK. [23](#)

Kadane, J. B., Meyer, M. M., and Tukey, J. W. (1999). Yule's association paradox and ignored stratum heterogeneity in capture-recapture studies. *Journal of the American Statistical Association*, 94:855–859. [24](#)

Karagiannis, I., Brandsema, P., and Van Der Sande, M. (2009). Warm, wet weather associated with increased legionnaires' disease incidence in the netherlands. *Epidemiology and Infection*, 137:181–187. [24](#)

Lai, C. C., Wang, C. Y., and Hsueh, P. R. (2020). Co-infections among patients with COVID-19: The need for combination therapy with non-anti-SARS-CoV-2 agents? *J. Microbiol Immunol Infect*, 53:505–512. [3](#)

Lettinga, K. D., Verbon, A., Weverling, G.-J., Schellekens, J. F. P., Boer, J. W. D., Yzerman, E. P. F., Prins, J., Boersma, W. G., van Ketel, R. J., Prins, J. M., and Speelman, P. (2002). Legionnaires' disease at a dutch flower show: prognostic factors and impact of therapy. *Emerg Infect Dis.*, 8:1448–1454. [3](#)

Martin, A. and Lemon, S. M. (2006). Hepatitis A virus: from discovery to vaccines. *Hepatology*. [4](#)

Matin, N., Grant, A., Granerod, J., and Crowcroft, N. (2006). Hepatitis a surveillance in england – how many cases are not reported and does it really matter? *Epidemiology and Infection*, 134:1299–1302. [28](#)

Nardone, A., Decladt, B., Jarraud, S., Etienne, J., Hubert, B., Infuso, A., Gallay, A., and Desenclos, J. C. (2003). Repeat capture–recapture studies as part of the evaluation of the surveillance of Legionnaires' disease in France. *Epidemiol Infect.*, 131:647–654. [4](#)

O'Hara, R. B., Lampila, S., and Orell, M. (2009). Estimation of rates of births, deaths, and immigration from mark-recapture data. *Biometrics*, (65):275–281. [2](#)

Otis, D. L., Burnham, K. P., White, G. C., and Anderson, D. R. (1978). Statistical inference from capture data on closed animal populations. *Wildlife Monographs: A Publication of Wildlife Society*, (62):3–135. [5](#), [8](#), [2](#)

Papoz, L., Balkau, B., and Lelleouch, J. (1996). Case counting in epidemiology: Limitations of methods based on multiple data sources. *International Journal of Epidemiology*, 25:474–478. [1](#)

Passer, J. K., Danila, R. N., Laine, E. S., Como-Sabetti, K. J., Tang, W., and Searle, K. M. (2020). The association between sporadic legionnaires' disease and weather and environmental factors, minnesota, 2011–2018. *Epidemiology and Infection*. [24](#), [25](#)

Rasch, G. (1961). On general laws and the meaning of measurement in psychology. *Proceedings of the Fourth Berkeley Symposium on Mathematical Statistics and Probability*, ed. J. Neyman, Berkeley, CA: University of California Press, 4.4:321–333. [5](#), [3](#)

Ruche, G. L., Dejour-Salamanca, D., Bernillon, O. P., Leparc-Goffart, I., Ledrans, M., Armengaud, A., Debruyne, M., Denoyel, G.-A., Brichler, S., Ninove, L., Després, P., and Gastellu-Etchegorry, M. (2013). Capture–recapture method for estimating annual incidence of imported dengue, France, 2007–2010. *Emerging Infectious Diseases*, 19:1740–1748. [2](#), [10](#)

Sanathanan, L. (1972). Estimating the size of a multinomial population. *The Annals of Mathematical Statistics*, 43:142–152. [8](#)

Stegelman, W. (1983). Expanding the Rasch model to a general model having more than one dimension. *Psychometrika*, 48:259–267. [4](#)

Tanner, M. A. and Wong, W. H. (1987). The calculation of posterior distributions by data augmentation. *Journal of the American Statistical Association*, 82:528–540. [11](#), [12](#)

Tsay, P. K. and Chao, A. (2001). Population size estimation for capture-recapture models with applications to epidemiological data. *Journal of Applied Statistics*, 28:25–36. [4](#), [5](#), [10](#)

Tsou, T., Liu, C., Huang, J., Tsai, K., and Chang, H. (2011). Change in hepatitis a epidemiology after vaccinating high risk children in taiwan, 1995-2008. *Vaccine*, 29(16):2956–2961. [27](#), [28](#)

Van Hest, N. A. H., Hoebe, C. J. P. A., Den Boer, J. W., Vermunt, J. K., Ijzerman, E. P. F., Boersma, W. G., and Richardus, J. H. (2008). Incidence and completeness of notification of

Legionnaires' disease in the Netherlands: covariate capture–recapture analysis acknowledging regional differences. *Epidemiol Infect*, 136:540–550. 3, 4, 5

Van Hest, R. (2007). *Capture-recapture methods in surveillance of Tuberculosis and other infectious diseases*. Print Partners Ipskamp, Enschede. 2

Wechsler, S., Izicki, R., and Esteves, L. G. (2013). A bayesian look at nonidentifiability: A simple example. *The American Statistician*, 67(2):1537–2731. 10

White, H. (1982). Maximum likelihood estimation of misspecified models. *Econometrica*, 50:1–25. 10

Wolter, K. M. (1986). Some coverage error models for census data. *Journal of the American Statistical Association*, 81:338–346. 23, 3

World Health Organization (2021). WHO Hepatitis A - Diagnosis. <https://www.who.int/news-room/fact-sheets/detail/hepatitis-a>. 27

Zaslavsky, A. M. and Wolfgang, G. S. (1993). Triple-system modeling of census, post-enumeration survey, and administrative-list data. *Journal of Business and Economic Statistics*, 11:279–288. 2

Zhou, F., Yu, T., Du, R., Fan, G., Liu, Y., Liu, Z., Xiang, J., Wang, Y., Song, B., Gu, X., Guan, L., Wei, Y., Li, H., Wu, X., Xu, J., Tu, S., Zhang, Y., Chen, H., and Cao, B. (2020). Clinical course and risk factors for mortality of adult inpatients with COVID-19 in Wuhan, China: A retrospective cohort study. *Lancet*, 395:1054–1062. 3

Web-based Supplementary Material for “Estimation of Population Size with Heterogeneous Catchability and Behavioural Dependence: Applications to Air and Water Borne Disease Surveillance” by Chatterjee and Bhuyan

A TRS Data Structure and Real Datasets

Table A.1: Data structure associated with a triple record system.

List 3								
List 1	In			Out			List 2	
	List 2			List 2				
	List 1	In	Out	Total	In	Out	Total	
In	x_{111}	x_{101}	$x_{1\cdot 1}$		x_{110}	x_{100}	$x_{1\cdot 0}$	
Out	x_{011}	x_{001}	$x_{0\cdot 1}$		x_{010}	x_{000}	$x_{0\cdot 0}$	
Total	$x_{\cdot 11}$	$x_{\cdot 01}$	$x_{\cdot\cdot 1}$		$x_{\cdot 10}$	$x_{\cdot 00}$	$x_{\cdot\cdot 0}$	

Table A.2: Dataset on Legionnaires’ disease (LD) and hepatitis A virus (HAV) surveillance.

Disease	Stratum	x_{111}	x_{110}	x_{101}	x_{011}	x_{100}	x_{010}	x_{001}	Total (x_0)
LD	All	155	31	131	45	56	30	332	780
	North	13	2	6	8	3	2	35	69
	East	45	3	42	7	13	13	62	185
	West	46	7	55	14	23	5	136	286
	South	51	19	28	15	13	9	99	234
HAV		28	21	17	18	69	55	63	271

B Existing Models and Estimates

As mentioned in Subsection 1.3 of the main article, modeling individual heterogeneity and list dependence is an important problem over the decades for its wide applications. In this section, we present frequently used models for TRS and associated estimates for the population size.

The assumptions associated with these models and their limitations in real applications are also discussed briefly. We consider these estimates to compare the performance of the proposed method through simulation study discussed in Section 4 of the main article.

B.1 Log-linear Model

Fienberg (1972b) and Bishop et al. (1975) discussed several log-linear models (LLMs) to account for list dependence using interaction effects. The general LLM under TRS is given by

$$\log(m_{ijk}) = u_0 + u_{1(i)} + u_{2(j)} + u_{3(k)} + u_{12(ij)} + u_{13(ik)} + u_{23(ik)} + u_{123(ijk)}, \quad (\text{B.1.1})$$

where $m_{ijk} = \mathbb{E}[x_{ijk}]$, $u_{l(0)} + u_{l(1)} = 0$, $u_{ll'(0j)} + u_{ll'(1j)} = 0$, $u_{ll'(i0)} + u_{ll'(i1)} = 0$, $u_{ll'l^*(0jk)} + u_{ll'l^*(1jk)} = 0$, $u_{ll'l^*(i0k)} + u_{ll'l^*(i1k)} = 0$, $u_{ll'l^*(ij0)} + u_{ll'l^*(ij1)} = 0$, for all $l, l', l^* = 1, 2, 3$, with $l \neq l' \neq l^*$ (Bishop et al., 1975, p.64). The parameters u_l , $u_{ll'}$ and u_{123} denote the main effects, pairwise interaction effects and the second order interaction effect for $l, l' = 1, 2, 3$. See Fienberg (1972a,b) and International Working Group for Disease Monitoring and Forecasting (1995) for more details. To ensure estimability of the model given in (B.1.1), one needs to consider $u_{123} = 0$, i.e. no second order interaction between lists. Under this assumption, the estimate of m_{000} is given by

$$\hat{m}_{000} = \frac{\hat{m}_{111}\hat{m}_{001}\hat{m}_{100}\hat{m}_{010}}{\hat{m}_{101}\hat{m}_{011}\hat{m}_{110}},$$

where \hat{m}_{ijk} is the maximum likelihood estimate of m_{ijk} assuming x_{ijk} to be a realization of an independent Poisson random variate for all (i, j, k) th cells, except the $(0, 0, 0)$ th cell. Finally, the estimate of N is obtained as $\hat{N}_{LLM} = x_0 + \hat{m}_{000}$ (Fienberg, 1972b). This is equivalent to the estimator proposed by Zaslavsky and Wolfgang (1993) with $\alpha_{EPA} = 1$. With additional assumption that $u_{12} = u_{13} = u_{23} = 0$, LLM in (B.1.1) reduces to independent model.

B.2 Time Behavioural Response Variation Model: M_{tb}

It is often observed in TRS that an individual's behavior changes in subsequent recapture attempts after the initial attempt. This change is known as behavioral response variation (Otis et al., 1978; Chatterjee and Mukherjee, 2016). When this behavioral response variation

is considered along with the assumption of list variation in capture probabilities, one would have a model known as M_{tb} model (Wolter, 1986). However, M_{tb} model does not account for the individual heterogeneity in capture probabilities.

Denote the first-time capture probability of any individual in the l -th list is by f_l for $l = 1, 2, 3$, and the recapture probability is denoted by c_l for $l = 2, 3$. Further, u_l and m_l denote, respectively, the number of first-time captured and recaptured individuals in the l -th list. Therefore, based on the the sufficient statistics ($u_1 = x_{1..}, u_2 = x_{01..}, u_3 = x_{001..}, m_2 = x_{11..}, m_3 = x_{101..} + x_{011..} + x_{111..}$) and the assumption of constant proportionality, i.e., $c_l/f_l = \phi$, for $l = 2, 3$, likelihood of the model M_{tb} is given by

$$L(N, \mathbf{f}, \phi) = \frac{N!}{(N - x_0)} f_1^{u_1} (1 - f_1)^{N - u_1} \phi^{m_2 + m_3} \prod_{l=2}^3 f_l^{u_l + m_l} (1 - f_l)^{N - M_{l+1}} (1 - \phi p_l)^{M_l - m_l},$$

where $x_0 = \sum_{i,j,k:ijk \neq 000} x_{ijk}$ and $M_l = u_1 + u_2 + \dots + u_{l-1}$ denote the total number of distinct captured individuals and the number of individuals captured at least once prior to the l -th attempt, respectively (Chatterjee and Bhuyan, 2020a). In this context, Chao et al. (2000) discussed various likelihood based methods for estimation of N . Note that, M_{tb} model does not utilize full information available from seven known cells in TRS, and hence, it loses efficiency in order to estimate N (Chatterjee and Bhuyan, 2020a). Moreover, the assumption of $c_2/f_2 = c_3/f_3 = \phi$ is not justifiable in various real life applications.

B.3 Models with individual heterogeneity

In educational statistics and Psychometry, Rasch model (Rasch, 1961) is widely used to account for the individual heterogeneity and list variation. The capture probabilities are model using logistic regression:

$$\log \left[\frac{\mathbb{E}[Z_h^{(l)}]}{1 - \mathbb{E}[Z_h^{(l)}]} \right] = v_h + s_l, \quad h = 1, 2, \dots, N; \quad l = 1, 2, 3, \quad (\text{B.3.1})$$

where v_h is a random effect representing the catchability of h th individual and s_l is effect of l th list. Even with the absence of behavioural response variation, dependence among the lists are induced is purely due to heterogeneity in capture probabilities (Chao et al., 2001). When we

set $v_h = 0$ in (B.3.1), the model reduces to multiple-recapture model with list independence. We now represent the Rasch model as a mixed effects generalized linear model that allows for individual heterogeneity and list variation in the following subsections.

B.3.1 Quasi-symmetry Model

The marginal cell probabilities for all the eight cells in a TRS can be represented as:

$$\log(p_{ijk}) = a + is_1 + js_2 + ks_3 + \gamma(i_+), \quad (\text{B.3.2})$$

where $i_+ = i + j + k$ and $\gamma(t) = \log[\mathbb{E}[\exp(v_h t) | i = j = k = 0]]$. See [Darroch et al. \(1993\)](#); [Fienberg et al. \(1999\)](#) for detailed derivation. Note that the term $\gamma(i_+)$ is invariant with respect to permutations of (i, j, k) , and hence the model in (B.3.2) is known as quasi-symmetry model (QSM) ([Darroch, 1981](#)). This is equivalent to the following assumption involving two constraints

$$p_{011}p_{100} = p_{101}p_{010} = p_{110}p_{001} \quad (\text{B.3.3})$$

which do not involve p_{000} . Therefore, an additional assumption is required, such as no second-order interaction exists. Under this assumption, the estimated count of the $(0, 0, 0)$ th cell is given by

$$\hat{x}_{000} = \frac{\hat{x}_{111}\hat{x}_{100}\hat{x}_{010}\hat{x}_{001}}{\hat{x}_{110}\hat{x}_{101}\hat{x}_{011}},$$

where \hat{x}_{ijk} is the maximum likelihood estimate of $\mathbb{E}[x_{ijk}|x_0]$ ([Darroch et al., 1993](#)).

B.3.2 Partial Quasi-symmetry Model

In many situations, the constraint provided in (B.3.3) associated with quasi-symmetry model is not realistic. However, it is reasonable to assume $p_{011}p_{100} = p_{101}p_{010}$ if $x_{011}x_{100}$ and $x_{101}x_{010}$ are close enough ([Darroch et al., 1993](#)). This condition implies that the patterns of heterogeneity are different for two different group of sources or lists as considered in generalized Rasch model proposed by [Stegelman \(1983\)](#). Under this assumption, the marginal cell probabilities can be represented as:

$$\log(p_{ijk}) = a + is_1 + js_2 + ks_3 + \gamma(i + j, k),$$

where $\gamma(t_1, t_2) = \log [\mathbb{E} [\exp(v_h t_1) \exp(z_h t_2) | i = j = k = 0]]$ with two nonidentically distributed random effects v_h and z_h associated with group of lists (L_1, L_2) and L_3 , respectively. This model is known as partial quasi-symmetry model (PQSM). See [Darroch et al. \(1993\)](#); [Fienberg et al. \(1999\)](#) for more details.

B.4 Sample Coverage Method

The idea of the sample coverage of a given sample is the probability weighted fraction of the population captured in that sample. The main principle relies on the fact that it is difficult to estimate the number of undercount directly, but the sample coverage can be well estimated in any non-independent situation with heterogeneous capture probability ([Chao et al., 1992](#); [Chao and Tsay, 1998](#)). In the context of TRS, the sample coverage is defined based on three hypothetical populations I, II, and III with capture probabilities $\{\mathbb{E} [Z_h^{(1)} | Z_h^{(2)}, Z_h^{(3)}] ; h = 1, \dots, N\}$, $\{\mathbb{E} [Z_h^{(2)} | Z_h^{(1)}, Z_h^{(3)}] ; h = 1, \dots, N\}$, and $\{\mathbb{E} [Z_h^{(3)} | Z_h^{(1)}, Z_h^{(2)}] ; h = 1, \dots, N\}$ corresponding to lists L_1 , L_2 , and L_3 , respectively. In particular, the sample coverage of first two lists $L_1 \cup L_2$ with respect to the population III is given by

$$C_{III}(L_1 \cup L_2) = \frac{\sum_{h=1}^N \mathbb{E} [Z_h^{(3)} | Z_h^{(1)}, Z_h^{(2)}] \mathbb{I}[Z_h^{(1)} + Z_h^{(2)} > 0]}{\sum_{h=1}^N \mathbb{E} [Z_h^{(3)} | Z_h^{(1)}, Z_h^{(2)}]}.$$

Similarly, one can obtain the sample coverages of other two possible combinations of samples, $C_{II}(L_1 \cup L_3)$ and $C_I(L_2 \cup L_3)$ with respect to the populations II and I, respectively. Now, the sample coverage of the three lists is defined as $C = \frac{1}{3} \{C_{III}(L_1 \cup L_2) + C_{II}(L_1 \cup L_3) + C_I(L_2 \cup L_3)\}$, and estimated by $\hat{C} = 1 - \frac{1}{3} \left[\frac{x_{100}}{n_1} + \frac{x_{010}}{n_2} + \frac{x_{001}}{n_3} \right]$. Finally, the estimator of N on based sample coverage approach is given by

$$\hat{N}_{sc} = \frac{x_{.11} + x_{1.1} + x_{11.}}{3\hat{C}} \left\{ 1 - \frac{1}{3\hat{C}} \left[\frac{(x_{1.0} + x_{.10})x_{11.}}{n_1 n_2} + \frac{(x_{10.} + x_{.01})x_{1.1}}{n_1 n_3} + \frac{(x_{0.1} + x_{01.})x_{.11}}{n_2 n_3} \right] \right\}^{-1}.$$

We refer this estimate as SC. From empirical studies, it is found that the performance of \hat{N}_{sc} is satisfactory if the sample coverage is over 55%. The performance also depends on the remainder term involved in the derivation of \hat{N}_{sc} , and the bias increases with its magnitude ([Chao and](#)

Tsay, 1998). Moreover, this method may produce infeasible estimates, i.e. $\hat{N}_{sc} < x_0$, unlike other methods.

C Derivations of Full Conditionals

The conditional posterior density of all the model parameters and latent variables are obtained from the joint posterior density of the unobserved quantities $\boldsymbol{\theta}$, \mathbf{y} , and \mathbf{b} provided in (5) and (6) of the main article.

C.1 Derivations of Full Conditionals of the Latent Cell Counts

The conditional posterior density of the latent cell counts \mathbf{y} , given $(N, \boldsymbol{\alpha}, \mathbf{b})$, is obtained as

$$\pi(\mathbf{y}|N, \boldsymbol{\alpha}, \mathbf{b}, \mathbf{x}) \propto \prod_{i,j,k=0,1} \pi(y_{ijk}|\boldsymbol{\theta}, \mathbf{b}, \mathbf{x}),$$

where

$$\begin{aligned} \pi(\mathbf{y}_{111}|\boldsymbol{\theta}, \mathbf{x}) &\propto \text{Multinomial}(x_{111}; Q_{111,1}^*, Q_{111,2}^*, Q_{111,3}^*, Q_{111,4}^*, Q_{111,5}^*), \\ \pi(y_{110,1}|\boldsymbol{\theta}, \mathbf{x}) &\propto \text{Binomial}(x_{110}; (1 - \alpha_0)\mathcal{P}_1\mathcal{P}_2(1 - \mathcal{P}_3)), \\ \pi(y_{011,1}|\boldsymbol{\theta}, \mathbf{x}) &\propto \text{Binomial}(x_{011}; (1 - \alpha_0)(1 - \mathcal{P}_1)\mathcal{P}_2\mathcal{P}_3), \\ \pi(y_{100,1}|\boldsymbol{\theta}, \mathbf{x}) &\propto \text{Binomial}(x_{100}; (1 - \alpha_0)\mathcal{P}_1(1 - \mathcal{P}_2)(1 - \mathcal{P}_3)), \\ \pi(y_{101,1}|\boldsymbol{\theta}, \mathbf{x}) &\propto \text{Binomial}(x_{101}; (1 - \alpha_0)\mathcal{P}_1(1 - \mathcal{P}_2)\mathcal{P}_3), \\ \pi(y_{010,1}|\boldsymbol{\theta}, \mathbf{x}) &\propto \text{Binomial}(x_{010}; (1 - \alpha_0)(1 - \mathcal{P}_1)\mathcal{P}_2(1 - \mathcal{P}_3)), \\ \pi(y_{001,1}|\boldsymbol{\theta}, \mathbf{x}) &\propto \text{Binomial}(x_{001}; (1 - \alpha_0)(1 - \mathcal{P}_1)(1 - \mathcal{P}_2)\mathcal{P}_3), \\ \pi(\mathbf{y}_{000}|\boldsymbol{\theta}, \mathbf{x}) &\propto \text{Multinomial}(N - x_0; Q_{000,1}^*, Q_{000,2}^*, Q_{000,3}^*, Q_{000,4}^*, Q_{000,5}^*), \end{aligned}$$

with $\mathbf{y}_{111} = (y_{111,1}, y_{111,2}, y_{111,3}, y_{111,4}, y_{111,5})$, $\mathbf{y}_{000} = (y_{000,1}, y_{000,2}, y_{000,3}, y_{000,4}, y_{000,5})$, $Q_{111,1}^* = (1 - \alpha_0)\mathcal{P}_1\mathcal{P}_2\mathcal{P}_3/Q_{111}$, $Q_{111,2}^* = \alpha_1\mathcal{P}_1\mathcal{P}_3/Q_{111}$, $Q_{111,3}^* = \alpha_2\mathcal{P}_1\mathcal{P}_2/Q_{111}$, $Q_{111,4}^* = \alpha_3\mathcal{P}_1\mathcal{P}_2/Q_{111}$, $Q_{111,5}^* = \alpha_4\mathcal{P}_1/Q_{111}$, $Q_{111} = (1 - \alpha_0)\mathcal{P}_1\mathcal{P}_2\mathcal{P}_3 + \alpha_1\mathcal{P}_1\mathcal{P}_3 + \alpha_2\mathcal{P}_1\mathcal{P}_2 + \alpha_3\mathcal{P}_1\mathcal{P}_2 + \alpha_4\mathcal{P}_1$; $Q_{000,1} = (1 - \alpha_0)(1 - \mathcal{P}_1)(1 - \mathcal{P}_2)(1 - \mathcal{P}_3)/Q_{000}$, $Q_{000,2} = \alpha_1(1 - \mathcal{P}_1)(1 - \mathcal{P}_3)/Q_{000}$, $Q_{000,3} = \alpha_2(1 - \mathcal{P}_1)(1 - \mathcal{P}_2)/Q_{000}$, $Q_{000,4} = \alpha_3(1 - \mathcal{P}_1)(1 - \mathcal{P}_2)/Q_{000}$, $Q_{000,5} = \alpha_4(1 - \mathcal{P}_1)/Q_{000}$, $Q_{000} = (1 - \alpha_0)(1 - \mathcal{P}_1)(1 - \mathcal{P}_2)(1 - \mathcal{P}_3) + \alpha_1(1 - \mathcal{P}_1)(1 - \mathcal{P}_3) + \alpha_2(1 - \mathcal{P}_1)(1 - \mathcal{P}_2) + \alpha_3(1 - \mathcal{P}_1)(1 - \mathcal{P}_2) + \alpha_4(1 - \mathcal{P}_1)$.

C.2 Derivations of Full Conditionals of the Random Effects

Note that the random effect b_l follows generalized logistic distribution of type-I with shape parameter δ_l , and its density function is given by

$$g_{b_l}(z|\delta_l) = \frac{\delta_l e^{-z}}{[1 + e^{-z}]^{\delta_l+1}}, -\infty < z < \infty, \delta_l > 0$$

for $l = 1, 2, 3$. Now, the conditional posterior density of b_1 is given by

$$\begin{aligned} \pi(b_1|\boldsymbol{\theta}, \mathbf{x}, \mathbf{y}) &\propto \mathcal{P}_1^{x_{1..}}(1 - \mathcal{P}_1)^{N-x_{1..}} \times g_{b_1}(z|\delta_1) \\ &= \left[\frac{1}{1 + e^{-b_1}} \right]^{x_{1..}} \left[\frac{e^{-b_1}}{1 + e^{-b_1}} \right]^{N-x_{1..}} \times \frac{\delta_1 e^{-b_1}}{[1 + e^{-b_1}]^{\delta_1+1}} \\ &\propto \frac{e^{-b_1[N-x_{1..}+1]}}{[1 + e^{-b_1}]^{N+\delta_1+1}} \\ &\equiv EGB2(n_1 + 1, m_1 + \delta_1), \end{aligned}$$

where $EGB2$ denotes exponential generalized beta distribution of second kind with parameters involving $m_1 = x_{1..}$, $n_1 = (N - x_{1..})$. Similarly, the conditional posterior densities of b_2 and b_3 can be obtained as

$$\begin{aligned} \pi(b_2|\boldsymbol{\theta}, \mathbf{x}, \mathbf{y}) &\propto EGB2(n_2 + 1, m_2 + \delta_2), \\ \pi(b_3|\boldsymbol{\theta}, \mathbf{x}, \mathbf{y}) &\propto EGB2(n_3 + 1, m_3 + \delta_3), \end{aligned}$$

respectively, where $m_2 = y_{111,1} + y_{111,3} + y_{111,4} + y_{110,1} + x_{011} + x_{010}$, $m_3 = y_{111,1} + y_{111,2} + y_{011,1} + y_{101,1} + x_{001}$, $n_1 = N - x_{1++}$, $n_2 = x_{100} + x_{101} + y_{001,1} + y_{000,1} + y_{000,3} + y_{000,4}$, and $n_3 = x_{110} + y_{100,1} + y_{010,1} + y_{000,1} + y_{000,2}$.

C.3 Derivations of Full Conditionals of the Dependence Parameter

The conditional posterior of $\boldsymbol{\alpha}$ is obtained as

$$\pi(\boldsymbol{\alpha}|\boldsymbol{\theta}_{-\boldsymbol{\alpha}}, \mathbf{x}, \mathbf{y}, \mathbf{b}) \propto \alpha_1^{k_1} \alpha_2^{k_2} \alpha_3^{k_3} \alpha_4^{k_4} (1 - \alpha)^{k_5} \times \pi(\boldsymbol{\alpha}),$$

where $k_1 = y_{111,2} + x_{110} - y_{110,1} + x_{001} - y_{001,1} + y_{000,2}$, $k_2 = y_{111,3} + x_{011} - y_{011,1} + x_{100} - y_{100,1} + y_{000,3}$, $k_3 = y_{111,4} + x_{101} - y_{101,1} + x_{010} - y_{010,1} + y_{000,4}$, $k_4 = x_{111} - \sum_{i=1}^4 y_{111,i} + N -$

$x_0 = \sum_{i=1}^4 y_{000,i}$, $k_5 = y_{111,1} + y_{110,1} + y_{011,1} + y_{100,1} + y_{101,1} + y_{010,1} + y_{001,1} + y_{000,1}$. Note that $\pi(\boldsymbol{\alpha}) \equiv Dirichlet(0.5, 0.5, 0.5, 0.5, 0.5)$ under prior choice I and the posterior distribution of $\boldsymbol{\alpha}$ is given by

$$\pi(\boldsymbol{\alpha} | \boldsymbol{\theta}_{-\boldsymbol{\alpha}}, \mathbf{x}, \mathbf{y}, \mathbf{b}) \sim Dirichlet(d_1, d_2, d_3, d_4, d_5),$$

where $d_u = k_u + 0.5$, for $u = 1, \dots, 5$.

Under prior choice II, $\pi(\boldsymbol{\alpha}) \equiv Dirichlet(\beta_1, \beta_2, \beta_3, \beta_4, \beta_5)$, and the posterior distribution of $\boldsymbol{\alpha}$ is given by

$$\pi(\boldsymbol{\alpha} | \boldsymbol{\theta}_{-\boldsymbol{\alpha}}, \mathbf{x}, \mathbf{y}, \mathbf{b}) \sim Dirichlet(d_1^*, d_2^*, d_3^*, d_4^*, d_5^*),$$

where $d_u^* = k_u + \beta_u$, for $u = 1, \dots, 5$.

C.4 Derivations of Full Conditionals of the Shape Parameter Associated with the Random Effects Distribution

Under the prior choice I, we consider the Jeffrey's prior for δ_l , i.e. $\pi(\delta_l) \propto \delta_l^{-1}$ for $l = 1, 2, 3$, and the conditional posterior distribution of δ_l is given by

$$\begin{aligned} \pi(\delta_l | \boldsymbol{\theta}_{-\delta_l}, \mathbf{x}, \mathbf{y}, \mathbf{b}) &\propto g_{b_1}(b_1 | \delta_1) \times \pi(\delta_l) \\ &\propto [1 + e^{-b_l}]^{-\delta_l} \\ &= e^{-\omega_l \delta_l} \\ &\propto Exponential(\omega_l), \end{aligned}$$

where $\omega_l = \log [1 + e^{-b_l}]$ for $l = 1, 2, 3$.

Under the prior choice II, $\pi(\delta_l) \propto Gamma(\gamma_l, \lambda_l)$ for $l = 1, 2, 3$. Then, the conditional posterior distribution of δ_l is given by

$$\begin{aligned} \pi(\delta_l | \boldsymbol{\theta}_{-\delta_l}, \mathbf{x}, \mathbf{y}, \mathbf{b}) &\propto g_{b_1}(b_1 | \delta_1) \times \pi(\delta_l) \\ &\propto [1 + e^{-b_l}]^{-\delta_l} \delta_l^{\gamma_l} e^{-\frac{\delta_l}{\lambda_l}} \\ &= e^{-\delta_l [\omega_l + \lambda_l^{-1}]} \delta_l^{\gamma_l} \\ &\propto Gamma(\gamma_l + 1, [\omega_l + \lambda_l^{-1}]^{-1}) \end{aligned}$$

for $l = 1, 2, 3$.

C.5 Derivations of Full Conditional of the Population Size

Note that Jeffrey's prior for N (i.e. $\pi(N) \propto N^{-1}$) is considered under both the prior choices I and II. The conditional posterior distribution of N given $(\boldsymbol{\theta}_{-N}, \mathbf{x}, \mathbf{y}_{-y_{000,5}}, \mathbf{b})$ is obtained as

$$\pi(N|\boldsymbol{\theta}_{-N}, \mathbf{x}, \mathbf{y}_{-y_{000,5}}, \mathbf{b}) \propto \frac{(N-1)!}{(N-x_0 - \sum_{u=1}^4 y_{000,u})!} [\alpha_4(1-\mathcal{P}_1)]^{N-x_0-\sum_{u=1}^4 y_{000,u}}.$$

To generate samples from the conditional posterior distribution of N , one can alternatively simulate from the conditional distribution of $y_{000,5} = N - x_0 - \sum_{u=1}^4 y_{000,u}$, given $(\boldsymbol{\theta}_{-N}, \mathbf{x}, \mathbf{y}_{-y_{000,5}}, \mathbf{b})$, provided as

$$\begin{aligned} \pi(y_{000,5}|\boldsymbol{\theta}_{-N}, \mathbf{x}, \mathbf{y}_{-y_{000,5}}, \mathbf{b}) &\propto \frac{(y_{000,5} + x_0 + \sum_{u=1}^4 y_{000,u} - 1)!}{y_{000,5}!} [\alpha_4(1-\mathcal{P}_1)]^{y_{000,5}} \\ &\propto NB\left(x_0 + \sum_{u=1}^4 y_{000,u}, 1 - \alpha_4(1-\mathcal{P}_1)\right), \end{aligned}$$

and then compute $N = y_{000,5} + x_0 + \sum_{u=1}^4 y_{000,u}$.

D Results from Simulation Study

The performance of the proposed estimators along with the existing competitors based on TRS data simulated from six choices of populations P1-P6 (See Table 1) with five different combinations of random-effects $\boldsymbol{\delta}$ as mentioned in Section 4 of the main article, is provided in the following tables. The abbreviation used in the tables are described below. Note that the CI corresponding to THBM refers to the HPD credible interval.

THBM: Trivariate Heterogeneous Bernoulli Model; SC: Sample Coverage; QSM: Quasi-symmetry Model; PQSM: Partial Quasi-symmetry Model; LLM: Log-linear Model, M_{tb} : Time Behavioural Response Variation Model; Independent: LLM without interaction effects.

Table D.1: Comparison of various estimators of the population size N under P1.

Model		$\delta = (1.6, 1.2, 0.8)$	$\delta = (1.3, 1.7, 0.9)$	$\delta = (1, 1.4, 1.8)$	$\delta = (0.8, 0.8, 0.8)$	$\delta = (1.6, 1.6, 1.6)$
$N = 200$						
THBM-I	\hat{N} (RMAE)	194 (0.070)	199 (0.070)	209 (0.086)	187 (0.106)	203 (0.063)
	CI	(164, 318)	(165, 329)	(166, 359)	(145, 354)	(172, 321)
	Coverage	96	99	99	96	99
THBM-II	\hat{N} (RMAE)	196 (0.050)	196 (0.050)	196 (0.051)	191 (0.079)	197 (0.041)
	CI	(168, 271)	(168, 263)	(168, 262)	(149, 315)	(174, 250)
	Coverage	99	99	99	99	99
SC	\hat{N} (RMAE)	175 (0.125)	176 (0.120)	180 (0.098)	163 (0.186)	183 (0.086)
	CI	(164, 187)	(164, 189)	(166, 198)	(146, 185)	(172, 194)
	Coverage	10	14	40	16	24
QSM	\hat{N} (RMAE)	191 (0.096)	209 (0.122)	288 (0.148)	194 (0.155)	238 (0.208)
	CI	(166, 263)	(170, 330)	(192, 631)	(149, 342)	(184, 415)
	Coverage	87	94	72	93	87
PQSM	\hat{N} (RMAE)	198 (0.105)	216 (0.139)	266 (0.343)	201 (0.173)	233 (0.186)
	CI	(167, 297)	(171, 365)	(184, 514)	(151, 366)	(182, 404)
	Coverage	92	96	83	92	91
LLM	\hat{N} (RMAE)	204 (0.120)	212 (0.132)	254 (0.292)	202 (0.189)	233 (0.188)
	CI	(169, 369)	(171, 405)	(182, 518)	(152, 414)	(181, 439)
	Coverage	84	84	78	82	81
M_{tb}	\hat{N} (RMAE)	240 (0.215)	237 (0.213)	262 (0.313)	256 (0.291)	249 (0.255)
	CI	(167, 471)	(167, 491)	(171, 563)	(147, 544)	(177, 494)
	Coverage	100	100	100	100	100
Independent	\hat{N} (RMAE)	166 (0.172)	3 165 (0.175)	165 (0.173)	146 (0.269)	173 (0.137)
	CI	(160, 170)	(159, 170)	(159, 172)	(138, 154)	(167, 177)
	Coverage	0	0	0	0	0
$N = 500$						
THBM-I	\hat{N} (RMAE)	487 (0.054)	499 (0.054)	522 (0.072)	472 (0.084)	519 (0.059)
	CI	(423, 729)	(425, 772)	(431, 815)	(381, 869)	(446, 783)
	Coverage	97	98	100	96	99
THBM-II	\hat{N} (RMAE)	489 (0.042)	490 (0.042)	493 (0.040)	481 (0.066)	494 (0.031)
	CI	(429, 642)	(330, 633)	(434, 636)	(391, 754)	(448, 604)
	Coverage	99	99	99	98	100
SC	\hat{N} (RMAE)	437 (0.126)	440 (0.120)	450 (0.100)	405 (0.191)	457 (0.086)
	CI	(419, 455)	(421, 460)	(427, 476)	(378, 436)	(440, 474)
	Coverage	0	0	7	0	2
QSM	\hat{N} (RMAE)	468 (0.075)	507 (0.068)	498 (0.077)	471 (0.104)	568 (0.140)
	CI	(427, 547)	(445, 633)	(427, 640)	(397, 625)	(483, 745)
	Coverage	77	95	94	89	77
PQSM	\hat{N} (RMAE)	485 (0.066)	528 (0.090)	515 (0.088)	473 (0.107)	567 (0.138)
	CI	(437, 612)	(456, 716)	(435, 704)	(401, 663)	(484, 774)
	Coverage	78	84	86	77	72
LLM	\hat{N} (RMAE)	495 (0.068)	514 (0.076)	500 (0.082)	474 (0.108)	566 (0.138)
	CI	(445, 598)	(448, 695)	(430, 712)	(404, 718)	(487, 839)
	Coverage	72	82	75	71	66
M_{tb}	\hat{N} (RMAE)	619 (0.239)	611 (0.224)	614 (0.230)	626 (0.251)	622 (0.244)
	CI	(418, 913)	(420, 919)	(398, 943)	(368, 989)	(441, 913)
	Coverage	100	100	100	100	100
Independent	\hat{N} (RMAE)	413 (0.174)	413 (0.175)	393 (0.215)	366 (0.268)	431 (0.137)
	CI	(404, 420)	(404, 420)	(383, 402)	(354, 378)	(424, 438)
	Coverage	0	0	0	0	0

Table D.2: Comparison of various estimators of the population size N under P2.

Model		$\delta = (1.6, 1.2, 0.8)$	$\delta = (1.3, 1.7, 0.9)$	$\delta = (1, 1.4, 1.8)$	$\delta = (0.8, 0.8, 0.8)$	$\delta = (1.6, 1.6, 1.6)$
$N = 200$						
THBM-I	\hat{N} (RMAE)	195 (0.067)	199 (0.070)	206 (0.080)	187 (0.102)	205 (0.062)
	CI	(165, 327)	(165, 329)	(165, 353)	(145, 349)	(173, 321)
	Coverage	98	99	99	97	100
THBM-II	\hat{N} (RMAE)	195 (0.049)	195 (0.049)	196 (0.050)	193 (0.081)	197 (0.039)
	CI	(168, 266)	(168, 262)	(168, 266)	(150, 318)	(175, 250)
	Coverage	99	99	99	99	99
SC	\hat{N} (RMAE)	175 (0.124)	175 (0.126)	179 (0.105)	162 (0.190)	183 (0.087)
	CI	(164, 188)	(164, 188)	(165, 195)	(145, 183)	(172, 194)
	Coverage	10	11	32	15	24
QSM	\hat{N} (RMAE)	203 (0.102)	203 (0.102)	248 (0.263)	195 (0.162)	235 (0.195)
	CI	(169, 306)	(169, 306)	(180, 475)	(150, 344)	(183, 406)
	Coverage	95	95	86	91	89
PQSM	\hat{N} (RMAE)	208 (0.119)	207 (0.116)	239 (0.227)	195 (0.157)	235 (0.197)
	CI	(169, 332)	(169, 325)	(177, 441)	(149, 345)	(182, 404)
	Coverage	94	94	90	93	90
LLM	\hat{N} (RMAE)	203 (0.113)	216 (0.150)	255 (0.300)	197 (0.170)	234 (0.200)
	CI	(169, 364)	(172, 405)	(180, 526)	(150, 406)	(183, 453)
	Coverage	84	83	78	82	81
M_{tb}	\hat{N} (RMAE)	224 (0.176)	216 (0.161)	242 (0.233)	232 (0.211)	230 (0.181)
	CI	(166, 452)	(166, 460)	(168, 540)	(145, 524)	(175, 470)
	Coverage	100	100	100	100	100
Independent	\hat{N} (RMAE)	166 (0.171)	166 (0.172)	165 (0.177)	146 (0.270)	173 (0.137)
	CI	(163, 174)	(160, 170)	(158, 170)	(139, 154)	(167, 177)
	Coverage	0	0	0	0	0
$N = 500$						
THBM-I	\hat{N} (RMAE)	492 (0.052)	506 (0.061)	524 (0.072)	473 (0.090)	519 (0.060)
	CI	(425, 770)	(427, 804)	(431, 822)	(381, 845)	(445, 786)
	Coverage	98	98	100	95	100
THBM-II	\hat{N} (RMAE)	490 (0.039)	493 (0.039)	493 (0.039)	482 (0.063)	494 (0.031)
	CI	(431, 645)	(432, 639)	(433, 637)	(391, 745)	(447, 602)
	Coverage	99	100	99	99	99
SC	\hat{N} (RMAE)	437 (0.125)	439 (0.123)	447 (0.106)	405 (0.190)	456 (0.089)
	CI	(419, 456)	(421, 458)	(425, 458)	(378, 436)	(439, 473)
	Coverage	0	0	2	1	2
QSM	\hat{N} (RMAE)	496 (0.063)	495 (0.063)	475 (0.079)	472 (0.103)	572 (0.148)
	CI	(441, 606)	(439, 605)	(418, 589)	(397, 626)	(484, 754)
	Coverage	93	94	88	89	75
PQSM	\hat{N} (RMAE)	509 (0.071)	502 (0.066)	479 (0.078)	473 (0.103)	571 (0.147)
	CI	(448, 661)	(444, 639)	(422, 622)	(401, 659)	(490, 794)
	Coverage	82	85	79	78	68
LLM	\hat{N} (RMAE)	496 (0.066)	518 (0.077)	603 (0.214)	475 (0.106)	569 (0.145)
	CI	(443, 666)	(447, 674)	(482, 881)	(404, 733)	(495, 885)
	Coverage	73	96	72	71	64
M_{tb}	\hat{N} (RMAE)	608 (0.219)	565 (0.151)	572 (0.165)	620 (0.241)	602 (0.206)
	CI	(416, 900)	(416, 866)	(394, 898)	(363, 979)	(437, 893)
	Coverage	100	100	100	100	100
Independent	\hat{N} (RMAE)	415 (0.171)	413 (0.173)	393 (0.213)	366 (0.268)	431 (0.137)
	CI	(406, 422)	(405, 421)	(383, 402)	(354, 377)	(424, 438)
	Coverage	0	0	0	0	0

Table D.3: Comparison of various estimators of the population size N under P3.

Model		$\delta = (1.6, 1.2, 0.8)$	$\delta = (1.3, 1.7, 0.9)$	$\delta = (1, 1.4, 1.8)$	$\delta = (0.8, 0.8, 0.8)$	$\delta = (1.6, 1.6, 1.6)$
$N = 200$						
THBM-I	\hat{N} (RMAE)	201 (0.059)	204 (0.065)	209 (0.086)	200 (0.092)	204 (0.055)
	CI	(170, 331)	(170, 335)	(166, 359)	(154, 390)	(177, 281)
	Coverage	98	99	99	98	98
THBM-II	\hat{N} (RMAE)	196 (0.050)	197 (0.049)	196 (0.050)	193 (0.075)	198 (0.039)
	CI	(172, 244)	(173, 241)	(168, 266)	(158, 269)	(178, 234)
	Coverage	97	98	99	96	97
SC	\hat{N} (RMAE)	175 (0.124)	184 (0.083)	186 (0.075)	176 (0.122)	188 (0.063)
	CI	(164, 188)	(170, 199)	(171, 203)	(155, 205)	(176, 200)
	Coverage	10	43	55	55	48
QSM	\hat{N} (RMAE)	199 (0.084)	205 (0.088)	288 (0.448)	207 (0.154)	225 (0.162)
	CI	(172, 272)	(174, 293)	(192, 631)	(159, 356)	(177, 390)
	Coverage	94	96	72	93	84
PQSM	\hat{N} (RMAE)	200 (0.084)	207 (0.102)	266 (0.343)	207 (0.149)	212 (0.095)
	CI	(172, 282)	(173, 306)	(184, 514)	(159, 355)	(180, 304)
	Coverage	94	95	83	95	95
LLM	\hat{N} (RMAE)	204 (0.095)	204 (0.099)	254 (0.292)	208 (0.155)	211 (0.096)
	CI	(174, 343)	(174, 341)	(182, 518)	(161, 409)	(181, 339)
	Coverage	85	82	78	86	84
M_{tb}	\hat{N} (RMAE)	218 (0.167)	214 (0.160)	262 (0.313)	227 (0.209)	226 (0.167)
	CI	(171, 466)	(171, 474)	(154, 340)	(154, 564)	(179, 481)
	Coverage	100	100	100	100	100
Independent	\hat{N} (RMAE)	173 (0.135)	173 (0.137)	165 (0.173)	157 (0.213)	178 (0.109)
	CI	(166, 179)	(166, 179)	(159, 172)	(148, 168)	(172, 183)
	Coverage	1	1	0	2	1
$N = 500$						
THBM-I	\hat{N} (RMAE)	504 (0.049)	512 (0.052)	522 (0.072)	505 (0.073)	510 (0.044)
	CI	(538, 779)	(440, 784)	(431, 815)	(405, 901)	(456, 626)
	Coverage	98	99	100	98	98
THBM-II	\hat{N} (RMAE)	491 (0.042)	494 (0.042)	495 (0.039)	485 (0.063)	498 (0.031)
	CI	(443, 574)	(445, 571)	(444, 582)	(412, 616)	(457, 561)
	Coverage	95	96	100	96	98
SC	\hat{N} (RMAE)	458 (0.083)	459 (0.082)	447 (0.106)	439 (0.122)	469 (0.063)
	CI	(437, 481)	(438, 482)	(424, 471)	(405, 480)	(451, 487)
	Coverage	10	11	4	20	16
QSM	\hat{N} (RMAE)	488 (0.052)	504 (0.055)	505 (0.067)	499 (0.091)	517 (0.057)
	CI	(444, 568)	(453, 602)	(442, 627)	(422, 655)	(468, 612)
	Coverage	92	95	95	93	98
PQSM	\hat{N} (RMAE)	493 (0.051)	511 (0.060)	511 (0.072)	500 (0.091)	517 (0.057)
	CI	(448, 594)	(458, 637)	(449, 670)	(427, 691)	(469, 623)
	Coverage	82	85	83	82	84
LLM	\hat{N} (RMAE)	501 (0.054)	505 (0.057)	502 (0.068)	502 (0.093)	516 (0.056)
	CI	(454, 644)	(458, 652)	(449, 690)	(433, 744)	(470, 681)
	Coverage	75	75	74	69	74
M_{tb}	\hat{N} (RMAE)	575 (0.164)	555 (0.148)	578 (0.182)	619 (0.239)	567 (0.149)
	CI	(426, 885)	(429, 871)	(410, 934)	(378, 1021)	(447, 874)
	Coverage	100	100	100	100	100
Independent	\hat{N} (RMAE)	431 (0.137)	432 (0.136)	416 (0.168)	393 (0.213)	446 (0.108)
	CI	(421, 441)	(421, 441)	(385, 401)	(378, 408)	(437, 554)
	Coverage	0	0	0	0	0

Table D.4: Comparison of various estimators of the population size N under P4.

Model		$\delta = (1.6, 1.2, 0.8)$	$\delta = (1.3, 1.7, 0.9)$	$\delta = (1, 1.4, 1.8)$	$\delta = (0.8, 0.8, 0.8)$	$\delta = (1.6, 1.6, 1.6)$
$N = 200$						
THBM-I	\hat{N} (RMAE)	192 (0.074)	195 (0.076)	192 (0.080)	183 (0.122)	194 (0.063)
	CI	(163, 320)	(163, 326)	(158, 332)	(141, 352)	(167, 297)
	Coverage	98	98	97	94	98
THBM-II	\hat{N} (RMAE)	197 (0.062)	197 (0.059)	197 (0.066)	190 (0.098)	198 (0.050)
	CI	(165, 287)	(165, 275)	(161, 286)	(144, 336)	(170, 268)
	Coverage	99	99	99	98	99
SC	\hat{N} (RMAE)	172 (0.139)	171 (0.144)	166 (0.172)	156 (0.221)	176 (0.118)
	CI	(162, 183)	(161, 182)	(153, 180)	(140, 175)	(167, 186)
	Coverage	4	3	3	6	5
QSM	\hat{N} (RMAE)	211 (0.125)	222 (0.164)	227 (0.186)	200 (0.172)	225 (0.162)
	CI	(169, 348)	(172, 391)	(169, 430)	(148, 387)	(177, 390)
	Coverage	96	94	96	94	94
PQSM	\hat{N} (RMAE)	200 (0.115)	212 (0.138)	254 (0.305)	205 (0.190)	226 (0.175)
	CI	(164, 318)	(166, 363)	(173, 523)	(147, 713)	(175, 408)
	Coverage	92	95	91	95	94
LLM	\hat{N} (RMAE)	204 (0.126)	208 (0.130)	244 (0.267)	205 (0.195)	226 (0.176)
	CI	(165, 373)	(166, 390)	(169, 501)	(148, 447)	(175, 439)
	Coverage	83	82	83	84	84
M_{tb}	\hat{N} (RMAE)	165 (0.180)	179 (0.146)	166 (0.186)	168 (0.217)	170 (0.155)
	CI	(159, 282)	(160, 378)	(154, 340)	(136, 384)	(165, 289)
	Coverage	83	100	92	94	88
Independent	\hat{N} (RMAE)	163 (0.186)	161 (0.195)	157 (0.213)	141 (0.294)	168 (0.161)
	CI	(158, 167)	(156, 165)	(152, 162)	(134, 148)	(163, 171)
	Coverage	0	0	0	0	0
$N = 500$						
THBM-I	\hat{N} (RMAE)	485 (0.064)	490 (0.064)	483 (0.064)	468 (0.101)	491 (0.049)
	CI	(418, 783)	(417, 790)	(408, 750)	(371, 866)	(430, 708)
	Coverage	97	98	99	95	99
THBM-II	\hat{N} (RMAE)	493 (0.054)	495 (0.051)	497 (0.057)	479 (0.084)	499 (0.043)
	CI	(424, 673)	(424, 649)	(416, 665)	(379, 791)	(436, 626)
	Coverage	99	99	99	98	99
SC	\hat{N} (RMAE)	430 (0.352)	429 (0.143)	414 (0.171)	390 (0.221)	441 (0.119)
	CI	(413, 446)	(412, 445)	(395, 435)	(365, 417)	(426, 456)
	Coverage	0	0	0	0	0
QSM	\hat{N} (RMAE)	514 (0.079)	541 (0.108)	551 (0.129)	491 (0.112)	548 (0.112)
	CI	(444, 659)	(456, 722)	(452, 762)	(399, 690)	(466, 723)
	Coverage	93	92	91	93	88
PQSM	\hat{N} (RMAE)	486 (0.074)	513 (0.082)	589 (0.192)	494 (0.116)	545 (0.110)
	CI	(430, 620)	(441, 686)	(473, 978)	(404, 777)	(466, 770)
	Coverage	79	85	72	83	79
LLM	\hat{N} (RMAE)	494 (0.075)	504 (0.078)	571 (0.158)	494 (0.116)	543 (0.109)
	CI	(438, 687)	(440, 701)	(464, 914)	(397, 723)	(460, 729)
	Coverage	71	73	77	94	91
M_{tb}	\hat{N} (RMAE)	422 (0.169)	457 (0.128)	472 (0.121)	490 (0.138)	445 (0.130)
	CI	(399, 539)	(399, 618)	(387, 722)	(340, 805)	(414, 590)
	Coverage	52	59	85	92	68
Independent	\hat{N} (RMAE)	407 (0.186)	406 (0.188)	393 (0.214)	353 (0.295)	419 (0.162)
	CI	(399, 414)	(398, 413)	(385, 401)	(342, 363)	(412, 424)
	Coverage	0	0	0	0	0

Table D.5: Comparison of various estimators of the population size N under P5.

Model		$\delta = (1.6, 1.2, 0.8)$	$\delta = (1.3, 1.7, 0.9)$	$\delta = (1, 1.4, 1.8)$	$\delta = (0.8, 0.8, 0.8)$	$\delta = (1.6, 1.6, 1.6)$
$N = 200$						
THBM-I	\hat{N} (RMAE)	189 (0.080)	193 (0.083)	195 (0.079)	179 (0.132)	197 (0.062)
	CI	(161, 291)	(160, 305)	(158, 321)	(140, 325)	(168, 299)
	Coverage	95	96	99	92	99
THBM-II	\hat{N} (RMAE)	196 (0.065)	196 (0.064)	197 (0.063)	191 (0.094)	198 (0.049)
	CI	(163, 293)	(163, 284)	(161, 286)	(144, 349)	(170, 267)
	Coverage	99	99	100	99	99
SC	\hat{N} (RMAE)	171 (0.145)	170 (0.149)	164 (0.181)	155 (0.225)	176 (0.120)
	CI	(161, 182)	(160, 181)	(151, 178)	(140, 174)	(166, 186)
	Coverage	2	2	4	6	5
QSM	\hat{N} (RMAE)	203 (0.114)	209 (0.130)	240 (0.240)	201 (0.175)	226 (0.171)
	CI	(167, 323)	(167, 346)	(173, 479)	(148, 389)	(177, 398)
	Coverage	94	93	92	95	93
PQSM	\hat{N} (RMAE)	203 (0.115)	210 (0.136)	242 (0.255)	207 (0.194)	226 (0.169)
	CI	(167, 385)	(167, 353)	(172, 470)	(149, 398)	(176, 391)
	Coverage	80	94	91	94	94
LLM	\hat{N} (RMAE)	205 (0.129)	211 (0.139)	241 (0.256)	208 (0.201)	226 (0.173)
	CI	(166, 377)	(168, 401)	(171, 489)	(150, 436)	(178, 446)
	Coverage	83	84	84	85	82
M_{tb}	\hat{N} (RMAE)	183 (0.120)	179 (0.130)	196 (0.101)	192 (0.136)	188 (0.101)
	CI	(161, 373)	(160, 378)	(159, 457)	(140, 465)	(168, 383)
	Coverage	99	100	100	100	100
Independent	\hat{N} (RMAE)	162 (0.189)	161 (0.195)	158 (0.211)	141 (0.294)	168 (0.162)
	CI	(157, 166)	(156, 165)	(152, 163)	(134, 148)	(163, 171)
	Coverage	0	0	0	0	0
$N = 500$						
THBM-I	\hat{N} (RMAE)	485 (0.057)	494 (0.059)	504 (0.061)	460 (0.097)	505 (0.050)
	CI	(417, 735)	(415, 727)	(411, 754)	(370, 787)	(431, 695)
	Coverage	96	99	100	93	100
THBM-II	\hat{N} (RMAE)	491 (0.056)	496 (0.053)	496 (0.051)	483 (0.086)	497 (0.043)
	CI	(421, 683)	(421, 680)	(417, 664)	(379, 818)	(435, 629)
	Coverage	98	99	99	99	99
SC	\hat{N} (RMAE)	426 (0.148)	425 (0.151)	409 (0.182)	388 (0.225)	440 (0.120)
	CI	(410, 442)	(408, 442)	(389, 429)	(363, 415)	(425, 455)
	Coverage	0	0	0	0	0
QSM	\hat{N} (RMAE)	496 (0.071)	507 (0.079)	568 (0.153)	489 (0.113)	546 (0.108)
	CI	(436, 620)	(439, 650)	(461, 799)	(398, 686)	(465, 718)
	Coverage	93	94	86	92	79
PQSM	\hat{N} (RMAE)	496 (0.072)	509 (0.081)	572 (0.158)	489 (0.114)	546 (0.108)
	CI	(437, 645)	(442, 682)	(470, 878)	(404, 733)	(470, 757)
	Coverage	83	79	76	80	80
LLM	\hat{N} (RMAE)	497 (0.073)	509 (0.081)	572 (0.160)	490 (0.115)	545 (0.108)
	CI	(441, 688)	(447, 743)	(475, 964)	(411, 803)	(476, 817)
	Coverage	73	72	71	70	71
M_{tb}	\hat{N} (RMAE)	453 (0.116)	458 (0.117)	493 (0.078)	521 (0.093)	474 (0.080)
	CI	(404, 693)	(402, 710)	(399, 812)	(347, 872)	(421, 725)
	Coverage	99	99	100	100	100
Independent	\hat{N} (RMAE)	406 (0.189)	403 (0.195)	395 (0.209)	352 (0.295)	419 (0.162)
	CI	(398, 412)	(395, 409)	(387, 403)	(341, 362)	(412, 425)
	Coverage	0	0	0	0	0

Table D.6: Comparison of various estimators of the population size N under P6.

Model		$\delta = (1.6, 1.2, 0.8)$	$\delta = (1.3, 1.7, 0.9)$	$\delta = (1, 1.4, 1.8)$	$\delta = (0.8, 0.8, 0.8)$	$\delta = (1.6, 1.6, 1.6)$
$N = 200$						
THBM-I	\hat{N} (RMAE)	194 (0.066)	200 (0.067)	207 (0.079)	191 (0.099)	203 (0.057)
	CI	(165, 317)	(166, 327)	(165, 363)	(146, 397)	(172, 347)
	Coverage	98	99	99	99	100
THBM-II	\hat{N} (RMAE)	195 (0.050)	196 (0.047)	196 (0.053)	192 (0.081)	196 (0.040)
	CI	(168, 270)	(169, 259)	(167, 265)	(150, 317)	(174, 248)
	Coverage	100	99	99	99	99
SC	\hat{N} (RMAE)	176 (0.122)	177 (0.116)	180 (0.103)	162 (0.190)	183 (0.086)
	CI	(164, 187)	(165, 190)	(165, 197)	(145, 184)	(172, 194)
	Coverage	10	15	35	16	25
QSM	\hat{N} (RMAE)	196 (0.095)	221 (0.152)	275 (0.384)	199 (0.168)	236 (0.203)
	CI	(167, 279)	(175, 371)	(188, 578)	(151, 361)	(183, 411)
	Coverage	90	94	77	91	87
PQSM	\hat{N} (RMAE)	195 (0.098)	222 (0.161)	277 (0.396)	195 (0.161)	238 (0.207)
	CI	(168, 319)	(178, 475)	(187, 542)	(149, 346)	(183, 410)
	Coverage	80	81	79	91	88
LLM	\hat{N} (RMAE)	204 (0.112)	214 (0.144)	253 (0.294)	197 (0.175)	237 (0.206)
	CI	(169, 364)	(172, 399)	(176, 504)	(150, 405)	(183, 453)
	Coverage	84	84	83	82	80
M_{tb}	\hat{N} (RMAE)	185 (0.109)	186 (0.104)	201 (0.091)	199 (0.116)	193 (0.083)
	CI	(165, 388)	(165, 407)	(166, 484)	(144, 496)	(173, 410)
	Coverage	100	100	100	100	100
Independent	\hat{N} (RMAE)	166 (0.168)	167 (0.167)	165 (0.176)	147 (0.267)	172 (0.139)
	CI	(161, 171)	(161, 171)	(158, 171)	(139, 155)	(167, 176)
	Coverage	0	0	0	0	0
$N = 500$						
THBM-I	\hat{N} (RMAE)	489 (0.052)	506 (0.059)	524 (0.073)	479 (0.086)	518 (0.057)
	CI	(424, 773)	(428, 807)	(431, 834)	(383, 882)	(446, 767)
	Coverage	98	99	100	98	100
THBM-II	\hat{N} (RMAE)	489 (0.041)	490 (0.040)	492 (0.039)	479 (0.067)	496 (0.031)
	CI	(431, 654)	(432, 624)	(433, 640)	(390, 729)	(448, 615)
	Coverage	99	99	100	98	99
SC	\hat{N} (RMAE)	437 (0.125)	443 (0.115)	450 (0.101)	405 (0.190)	457 (0.086)
	CI	(420, 455)	(424, 462)	(426, 475)	(378, 436)	(440, 474)
	Coverage	0	1	7	1	3
QSM	\hat{N} (RMAE)	480 (0.065)	533 (0.090)	653 (0.307)	473 (0.100)	571 (0.149)
	CI	(433, 570)	(458, 685)	(509, 964)	(398, 628)	(484, 752)
	Coverage	87	93	50	90	75
PQSM	\hat{N} (RMAE)	479 (0.067)	534 (0.094)	657 (0.314)	473 (0.101)	571 (0.149)
	CI	(434, 582)	(461, 719)	(519, 1042)	(402, 661)	(487, 780)
	Coverage	78	82	49	80	67
LLM	\hat{N} (RMAE)	496 (0.065)	515 (0.077)	601 (0.207)	476 (0.102)	569 (0.147)
	CI	(445, 687)	(453, 713)	(492, 993)	(409, 740)	(490, 850)
	Coverage	72	77	63	73	66
M_{tb}	\hat{N} (RMAE)	464 (0.100)	499 (0.069)	522 (0.053)	523 (0.087)	498 (0.053)
	CI	(411, 722)	(414, 785)	(414, 869)	(358, 899)	(433, 774)
	Coverage	100	100	100	100	100
Independent	\hat{N} (RMAE)	415 (0.171)	416 (0.169)	411 (0.178)	366 (0.267)	431 (0.138)
	CI	(406, 422)	(407, 423)	(401, 421)	(354, 378)	(423, 438)
	Coverage	0	0	0	0	0